

Do we have two hearts? New insights in right ventricular function supported by myocardial imaging echocardiography

Antonio Vitarelli · Claudio Terzano

Published online: 29 October 2009
© Springer Science+Business Media, LLC 2009

Abstract RV performance is difficult to evaluate, given its geometry, interrelationship with the left ventricle, and sensitivity to alterations in pulmonary pressure. This article focuses on some of the challenges related to the assessment of RV function in the setting of the RV's unique anatomic, physiologic, conventional and newer echocardiographic aspects, and therapeutic implications. The majority of proposed methods of echocardiographic assessment of RV function are based on volumetric approximations of the RV. Such approaches have inherent limitations, first as volume-related measures such as EF are load dependent, second because of the complex geometry of the RV. The issue of RV geometry is usually overcome using geometry-independent parameters such as tricuspid annular excursion and the Tei index. The recent introduction of real-time three-dimensional echocardiography and myocardial imaging echocardiography (tissue Doppler imaging, 1D-strain and 2D-strain echocardiography) implied a great progress in echocardiography. Tissue Doppler imaging allows the quantitative assessment of RV systolic and diastolic function by means of measurement of myocardial velocities. Strain measurements have been shown to correlate well with sonomicrometry segment length measurements both in the inflow and outflow tract of the RV and under different loading conditions. Other findings have been reported in chronic and acute clinical settings. Standard and novel echocardiographic methods of assessment of RV size

and performance can help clinicians in the treatment of acute and chronic RV failure and contribute to a better understanding of the peculiar chamber-related functional mechanisms in the context of ventricular interdependent independency.

Keywords Right ventricular function · Echocardiography · Tissue Doppler imaging · Speckle tracking imaging · Three-dimensional echocardiography

Introduction

In the last two decades, there has been an increasing interest in the right ventricle (RV) particularly with regard to right ventricular failure. The assessment of RV function has become important in the management of pulmonary hypertension, right ventricular cardiomyopathies, cardiac transplantation, subpulmonary or systemic RV dysfunction in congenital heart disease, and left ventricular dysfunction. This chamber, at times termed “the forgotten ventricle”, is no more considered an “unnecessary” part of the normal circulation or regarded as a “passive” conduit.

The mechanisms of ventricular function have been studied in animal models and in human beings, mostly pointing to left ventricular (LV) physiology. RV performance is difficult to evaluate, given its geometry, interrelationship with the left ventricle, and sensitivity to alterations in pulmonary pressure. With recent advances in Doppler and Doppler tissue echocardiography, new methods for measuring regional and global RV function or contractility have been suggested, but knowledge of the impact of changes in loading conditions on these parameters in RV function of human beings is limited.

A. Vitarelli (✉)
Echocardiology Unit, Cardio-Thoracic Department,
Sapienza University, Via Lima 35, 00198 Rome, Italy
e-mail: vitar@tiscali.it

C. Terzano
Pneumology Unit, Cardio-Thoracic Department,
Sapienza University, Rome, Italy

The goal of this article is to focus on some of the challenges related to the assessment of RV function in the setting of the RV's unique anatomic, physiologic, conventional and newer echocardiographic aspects, and therapeutic implications.

RV structure and musculature

Because RV normally operates at a lower pressure than the LV, it is more thin walled and compliant on the basis of the Laplace relationship, and its septal contour is indented by the dominant LV, producing a complex shape that is difficult to model geometrically (Fig. 1a). Whereas, the LV presents with an ellipsoidal shape, the RV appears triangular when viewed from the side and crescent shaped when viewed in cross section. The geometry of the RV is also influenced by the position of the interventricular septum

that is concave toward the LV in both systole and diastole under normal loading and electrical conditions.

The RV is distinguished from LV by having coarser trabeculae, a moderator band, and a lack of fibrous continuity between the inlet and outflow valves. The cavity of the RV chamber can be described [1] in terms of three component parts (Fig. 1b): inlet, trabeculated apical myocardium, and outlet (infundibulum or conus). In the analysis of congenitally malformed hearts, this tripartite concept is more useful than the traditional division of the right ventricle into sinus and conus components [2]. The apical trabecular component allows direct distinction between morphologically right, left, or indeterminate ventricles irrespective of the location of the chamber within the ventricular mass. The muscular trabeculations in the apical part of the morphologic RV are coarse, whereas the apical trabeculations of the LV are fine and display a crisscross pattern. The inlet portion is the RV portion

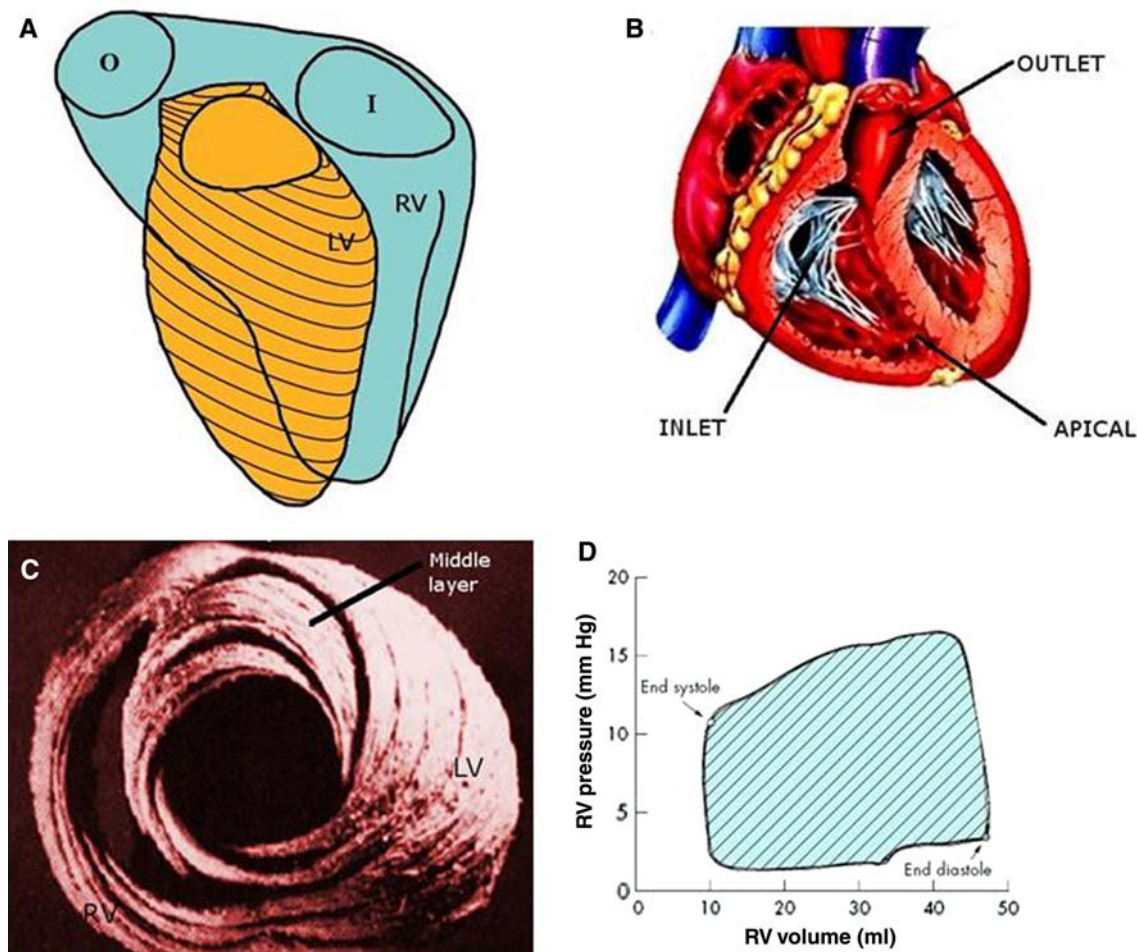


Fig. 1 RV anatomy and physiology. **a** RV complex shape compared to ellipsoid LV shape. **b** Three component parts of RV inside cavity: inlet, apical trabecular, and outlet. **c** RV and LV wall fibers layers. The LV middle layer is shown (absent in the RV). **d** RV pressure/

volume loop. The RV has the same stroke volume compared to the LV but with approximately 25% of stroke work (*dashed area under the curve*). I = inlet chamber; O = outlet chamber

containing the tricuspid valve, chordae tendineae, and papillary muscles. The subpulmonary infundibulum is the anterosuperior muscular tube that leads to the pulmonary valve and is usually free of muscular trabeculations. Proximally, however, a clear cut demarcation between outlet and apical portions is absent since trabeculations running from the septum to the parietal wall are frequently found [3].

The musculature of ventricular wall is composed of multiple layers that form a complex three-dimensional network of myocytes in a matrix of fibrous tissue [3, 4]. The superficial myofibers are arranged circumferentially in the subepicardium in a direction that is parallel to the atrioventricular groove and encircle the subpulmonary infundibulum. At the right ventricular apex, superficial myofibers invaginate in spiral fashion to form the deep or subendocardial myofibers that are aligned longitudinally toward the base. In the normal heart, the muscular wall of the right ventricle not including trabeculations is 3–5 mm thick. In this, relatively thin wall circumferential and longitudinal orientations predominate. In contrast, the thicker left ventricular wall contains obliquely oriented myofibers superficially, longitudinally oriented myofibers in the subendocardium, and predominantly circular fibers in between.

Dissection studies showed that myocardial fibers course in a helical continuum between the subendocardium and subepicardium. The LV has a middle layer (Fig. 1c) containing circumferential constrictor fibers that provide the main driving force of the LV by reducing ventricular diameter. A further contribution to LV ejection is the shortening of the ventricle through contraction of its oblique fibers. A third component of ejection is torsion, rotation of the LV apex relative to the base. The RV also has helical fibers and undergoes torsion. However, the RV lacks a middle layer and must rely more heavily on longitudinal shortening than does the LV. The RV contracts in a “peristaltic” pattern [3] that proceeds from the sinus (oblique fibers with an average major radius of curvature) to the infundibulum (circumferential fibers with a small radius of curvature).

RV physiology

Under normal circumstances, the RV is connected in series with the LV and is, therefore, obligated to pump the same effective stroke volume. The RV has a unique physiology related to the low hydraulic impedance characteristics of the pulmonary vascular bed. Compared with the systemic circulation, pulmonary circulation has a much lower vascular resistance, greater pulmonary artery distensibility, and a lower peripheral pulse wave reflection coefficient.

Right-sided pressures are lower than left-sided pressures, and RV pressure tracings show an early peaking and a rapidly declining pressure. Since RV systolic pressure exceeds rapidly the low pulmonary artery diastolic pressure, RV isovolumic contraction time is shorter.

There are some data [3–5] to suggest that the myocardium of the RV itself is intrinsically different to that of the LV (faster twitch velocity in isolated RV muscle bundles). The RV shortens in a circumferential direction during the isovolumic contraction (controlled by subepicardial fibers) and longitudinally during the ejection phase (controlled by subendocardial fibers). RV contraction is sequential. It starts with a short contraction of the inlet region and ends with the contraction of the infundibulum that is of longer duration. Since the onset of the RV ejection at outflow tract occurs 25–50 ms after the contraction of the inflow tract, this results in overall peristaltic ventricular motion. Thus, the RV contracts by three separate mechanisms: inward movement of the free wall (bellows effect), contraction of the longitudinal fibers (long axis shortening), and traction on the free wall at the points of attachment secondary to LV contraction. Global RV shortening is greater longitudinally than radially.

The characteristics of RV contraction are largely dependent on its loading conditions. RV output approximates that of the left (the same stroke volume) but with approximately 25% of stroke work (less energy cost). This is not only because of the low pressure pulmonary system but also because of the unique characteristics of the RV pressure–volume relationship (Fig. 1d).

Human RV pressure–volume relationships were defined recently [6]. Using biplane angiograms with simultaneous pressure measurements, the normal RV pressure–volume relationship was defined as a triangular or trapezoidal form, with ill-defined periods of isovolumic contraction and particularly isovolumic relaxation. This pattern has subsequently been confirmed by other authors [7, 8].

Pressure–volume loops help to understand the complex relationship between RV contractility, preload, and afterload, since they may depict instantaneous pressure–volume curves under different loading conditions. It has been shown [9] that the LV end-systolic pressure–volume relationship can be approximated by a linear relationship. Ventricular elastance represents the slope of this relationship. Many investigators consider ventricular elastance as the most reliable index of contractility in virtue of its relative load independence. Also, the RV, despite having markedly different ventricular geometry and hemodynamics, follows a time-varying elastance model. Whereas in LV pressure–volume interpretation the end-systolic elastance is commonly used as index of contractility, maximal RV elastance better reflects RV contractility due to the different shape of the RV pressure–volume curve.

The normal maximal RV elastance has been reported 1.30 ± 0.84 mm Hg/ml [10].

Some limitations in the RV time-elastance model have been reported [11], such as variability in slope values and afterload dependency. RV afterload represents the load that the RV has to overcome during ejection. Compared with the LV, the RV shows higher sensitivity to afterload change. Pulmonary vascular resistance (PVR) may not reflect the complex nature of ventricular afterload, although in clinical practice, it is the most commonly used index of afterload. Ideally, a more complete model should take into account the static and dynamic components of pulmonary vascular impedance and valvular or intracavitary resistive components [12, 13].

Another important factor must be taken into account when assessing both the normal and abnormal right heart circulation. The influence of the mechanical work of breathing has a major impact on beat-by-beat and breath-by-breath right heart hemodynamics. With each inspiration, the small change in intrapleural pressure (2–5 cm H₂O) leads to a significant increase in venous return and RV preload. This accounts for the changes of RV stroke volume during the respiratory cycle (waxing and waning). The opposite phenomenon (a fall in RV stroke volume as mean airway pressure increases) is partially due to changes in preload.

The regulation of RV function as well as LV function is based on the mechanisms that include heart rate, the Frank–Starling mechanism, and the autonomic nervous system. The autonomic nervous system has a differential effect on the inflow and outflow region of the RV, since vagal stimulation prolongs the normal sequence of inflow–outflow contraction, while sympathetic stimulation may abolish the usual delay or even reverse this sequence. Moreover, animal and human studies have suggested that the inotropic response of the infundibulum to sympathetic activation may be greater than that of the inflow tract [13].

The perfusion of the RV has some peculiar aspects [12, 13]. The blood supply of the RV varies according to the dominance of the coronary system. In a right-dominant system, which is found in approximately 80% of the population, the right coronary artery (RCA) supplies most of the RV. The relative resistance of the RV to irreversible ischemic injury may be explained by several factors. The RV has a more favorable oxygen supply–demand profile than the LV, because oxygen demand is lower, since RV free wall has less myocardial mass and faces lower preload and afterload. Less oxygen extraction at rest imparts to the RV greater extraction reserve capabilities during stress. RV perfusion also is more favorable, in part because of a dual anatomic supply system as approximately one-third of RV-free wall flow is derived from left coronary branches. In addition, because the RV-free wall is thinner, develops lower systolic intramyocardial pressure and faces less

diastolic intracavitary pressure, it receives relatively homogeneous transmural perfusion in systole as well as diastole, both under physiologic conditions and with collateral perfusion during RCA occlusion. Furthermore, there is a comparatively greater likelihood of acute collateral development to the RCA, attributable in part to lower coronary resistance that favors a left-to-right transcoronary pressure gradient.

RV pathophysiology

The right ventricle tolerates volume overload better than pressure overload and therefore may remain well adapted to right-sided valvular regurgitant lesions for extended periods of time. In atrial septal defect and tricuspid regurgitation, the RV may tolerate volume overload for a long time without a significant decrease in RV systolic function. In contrast to volume-overload states, moderate to severe acquired pulmonary arterial hypertension (PAH) in the adult often leads to RV dilatation and failure and may also lead to RV ischemia, which may further aggravate ventricular dysfunction. In acute pressure-overload states such as pulmonary embolism, a patient with a previously normal RV is incapable of acutely generating a mean pulmonary artery pressure >40 mm Hg, and RV failure occurs early in the presence of a significant embolic burden.

Two examples of otherwise well tolerated chronic pressure-overload states include Eisenmenger syndrome and congenital pulmonary stenosis [13–15]. In pulmonary hypertension associated with initial left-to-right shunt, the lesion may remain minimally symptomatic during the high-volume phase, until pulmonary vasculopathy develops and the shunt reverses (Eisenmenger's phenomenon). Even after Eisenmenger's physiology is well established, the outlook for these patients is better than for patients with idiopathic pulmonary arterial hypertension, perhaps because of preconditioning by the prior volume load or retention of fetal right heart phenotype characteristics [14, 15]. In congenital pulmonary valve stenosis, the degree of ventricular hypertrophy varies with the severity of obstruction, and the RV usually adapts well to pulmonary valve stenosis even when severe, with symptoms being unusual in children and adolescents. Less frequently long-standing untreated severe obstruction may lead to RV failure and tricuspid regurgitation.

An initial adaptive response of myocardial hypertrophy to pressure overload is followed by progressive contractile dysfunction. Subsequent chamber dilatation allows compensatory preload and maintains stroke volume despite reduced fractional shortening. As contractile weakening progresses, clinical evidence of decompensated RV failure occurs, characterized by rising filling pressures, diastolic

dysfunction, and diminishing cardiac output, which is worsened by tricuspid regurgitation due to annular dilatation and poor leaflet coaptation. Both RV diastolic dysfunction and tricuspid regurgitation may accentuate right-to-left shunting through a patent foramen ovale and lead to hypoxemia. The increased size and pressure overload of the RV also produce diastolic dysfunction of the LV and impose an additional cause of symptoms [16, 17].

The specific mechanisms underlying the development of RV failure secondary to pulmonary hypertension are not well understood. It is unclear why some patients develop RV myocardial ischemia or myocytes undergo apoptosis, or if there is microvascular endothelial cell dysfunction. In end-stage pulmonary hypertension, the shape of the RV is changed from the normal conformation, and RV wall stress and free wall thickness are inversely related [17]. Plasma levels of brain natriuretic peptide and troponin T correlate with pulmonary arterial pressure and pulmonary vascular resistance in patients with pulmonary arterial hypertension. Increases in brain natriuretic peptide plasma levels during serial follow-up visits are associated with increased mortality in patients with idiopathic pulmonary arterial hypertension, but paradoxically atrial natriuretic peptides may promote cardiomyocyte survival. RV failure cannot be understood simply by extrapolating hemodynamic and clinical data from LV failure. It appears that the ventricles are categorically different in spite of ventricular interdependence, and that these differences may have implications in the assessment and treatment of patients with predominantly right, left, or biventricular heart failure.

Genetic and embryologic cardiac investigations have shown that RV and LV originate from different progenitor cells and different sites. LV and atrial chambers arise from the primary heart field, RV, and RVOT from the cells of the anterior heart field. The sinus part of the RV is derived from the ventricular portion of the primitive cardiac tube, whereas the infundibulum is derived from the conus cordis. The discovery of 2 chamber-restricted basic helix-loop helix transcription factors, HAND1 and HAND2, and studies of knockout mice led to the recognition of chamber-specific gene expression with different transcriptional events leading to RV and LV formation [18, 19]. The transcription factor Bop is recognized as a regulator of RV development and a transcriptional target of myocyte enhancer factor 2C. GATA4 is required for HAND2 expression and RV formation. RV wall thickness in pulmonary arterial hypertension has a variable degree, and there is evidence for changes of gene expression in the pressure-overloaded failing right ventricle (fetal gene pattern recapitulation, decreased α -myosin heavy chain gene, and increased expression of fetal β -myosin heavy chain). The clinical experience that some patients with

cardiomyopathy or pulmonary arterial hypertension develop RV failure earlier than others as assessed by RV filling pressure at the time of diagnosis has suggested that there may be a genotypic difference between patients. Other observations have suggested the concept of genetically controlled RV hypertrophy [20].

The mechanisms by which LV failure leads to RV dysfunction are also not completely clear. Congestive heart failure affects lung mechanics and gas exchange and pulmonary function abnormalities consist of reduction in lung volumes, decreased lung compliance, and restrictive lung physiology. The reduced alveolar-capillary membrane diffusing capacity is not reversible, demonstrating the clinical importance of lung structural remodeling in heart failure. The lungs from animal models of heart failure and from humans with pulmonary venous hypertension show septal thickening, myofibroblast proliferation, and interstitial matrix deposition [17]. Their physical and biological determinants as well as the impact on RV failure development are still being investigated.

Ventricular interdependence

The meaning of ventricular interdependence is that the size, shape, and compliance of one ventricle may affect the size, shape, and pressure–volume relationship of the other ventricle through direct mechanical interactions. It is always present but most apparent with changes in loading conditions such as those seen with respiration or sudden postural changes. It plays an important role in the pathophysiology of RV failure, especially in the acute setting.

Many experimental and clinical studies confirmed the mechanism of the diastolic ventricular interdependence [12, 21–23]. Right ventricular diastolic dysfunction adversely affects LV diastolic properties through diastolic interactions mediated by the reversed curved septum and exacerbated by elevated intrapericardial pressure. In acute RV pressure or volume overload [12, 22], elevated RV diastolic pressure and RV dilation push the interventricular septum toward the underloaded left ventricle, limiting LV filling and elevating intrapericardial pressure. The pericardial constraint further impairs both RV and LV compliance and filling, whereas on the other hand, LV volume or pressure overload may contribute to shift upward the RV diastolic pressure–volume relationship and redistribute RV filling into late diastole.

Assessment of ventricular interdependence is helpful in differentiating restrictive from constrictive physiology [23], both of which can present with right-sided heart failure. Ventricular interdependence may be clinically assessed by considering the degree of reciprocal respiratory change in ventricular filling profiles, ventricular coupling (in dimension or pressure), or abnormal septal motion.

Interventricular septum

The role of the septum in the ventricular–ventricular interaction is not fully determined [24–33]. Some authors have suggested that this interaction is caused by the shared septal wall, whereas others have suggested that the free walls affect the contralateral ventricle independently of the septum [27, 28]. A previously described model [30] showed the impact of septal impairment on ventricular pressure development. To better understand the interaction of the right-sided and left-sided part of the septum, a geometrical model has been developed evaluating the transmural gradients in stress and strain of the left ventricle and the IVS [31]. This showed that the right and left sides of the septum respond differently to various conditions such as a one-sided pressure increase by alternate aortic and pulmonary arterial constrictions.

The development of tissue Doppler imaging allowed for evaluation of the differences in regional function within the septum. With the development of echocardiographic equipment and techniques, a bright line in the IVS became constantly detectable, which separates the left from the right side of the septum. Functional differences such as differences in thickening, strain, and strain rate of both sides of the septum have not been completely studied, though nonlinear contraction throughout the myocardium is suggested by the differing behaviors of longitudinal and circumferential fibers.

A recent study [32] showed that the septum can be consistently divided into a left and a right side based on a bright echocardiographic signal. Also, differences in thickening and radial strain between the two sides are observable. These differences are not present in longitudinal motion. Knowledge of fiber architecture with an abrupt change in the middle of the septum, together with the discussed cases, suggests the septum to be a morphologically and functionally bilayered structure potentially supplied by different coronary arteries.

The transverse geometry of the RV free wall allows constriction (bellows-type motion), whereas oblique septal fiber orientation and midline septal position are essential for ventricular twisting, the vital mechanism for RV ejection against increased pulmonary vascular resistance. Therefore, the septum is considered “the lion or motor of RV performance” [33]. Distortion of such normal structure/function relationships underlies the pathophysiologic mechanisms of RV failure.

Echocardiographic assessment of right ventricular function

Echocardiography is used as the first-line imaging modality for the assessment of RV size and function because of its

availability. The quantitative assessment of RV size and function is often difficult, because of the complex anatomy, chamber’s crescentic shape, separate infundibulum, and prominent trabeculation. While detailed functional assessment of the outflow tract and the apical “trabecular” compartment may be difficult to achieve by echocardiography, that of the inflow tract could easily be imaged and studied by all echocardiographic modalities. However, when used in a qualitative fashion, two-dimensional echocardiography can easily obtain valuable information about RV size and function.

For qualitative evaluation, the RV size should be compared with the LV size. In the parasternal long axis and apical four-chamber views, the normal RV is approximately two-thirds the size of the LV. If the RV appears larger than the LV and/or shares the apex, RV dilatation may be present.

Confirmation in other views is needed to avoid false positive findings. Because of the complex shape of the right ventricle, triangular from the frontal aspect and crescentic from the apex, it is necessary to image the right ventricle from several projections, each characterized by specific anatomic landmarks (Fig. 2). From short-axis projections, the RV should be smaller than the LV, while the LV shape should have a circular geometry throughout the cardiac cycle. The RV should also be evaluated from the subcostal views. If the RV appears larger in length or diameter, RV dilatation is likely to be present. Finally, the transesophageal (TEE) approach can be used in assessing the RV in congenital heart disease, but also may be very useful in adult patients with difficult transthoracic windows. It gives four-chamber planes and planes that display the RVOT longitudinally (Fig. 2e, i).

RV size and function can also be quantitatively assessed (Table 1) by tracing the RV endocardial border or measuring RV dimensions [34–42]. However, interobserver variability is high. The American Society of Echocardiography (ASE) published the recommendations for RV and RV outflow tract assessment as part of its guidelines on chamber quantitation [36]. The problematic nature of systolic function assessment due to “the complex geometry of the RV and the lack of standard methods for assessing RV volumes” was recognized and discussed in this ASE document. Comparisons between 2D echocardiography and MRI for linear and cross sectional area measurements of the RV have been performed on normal subjects [40] and on patients with end-stage lung disease [41] and congenital heart disease and RV volume overload [42].

A wide variety of techniques for the measurement of RV ejection fraction (RVEF) have been proposed, but none is currently considered as the gold standard [43–47]. Two-dimensional assessment of RVEF with Simpson’s rule and the area–length method showed moderate correlation with

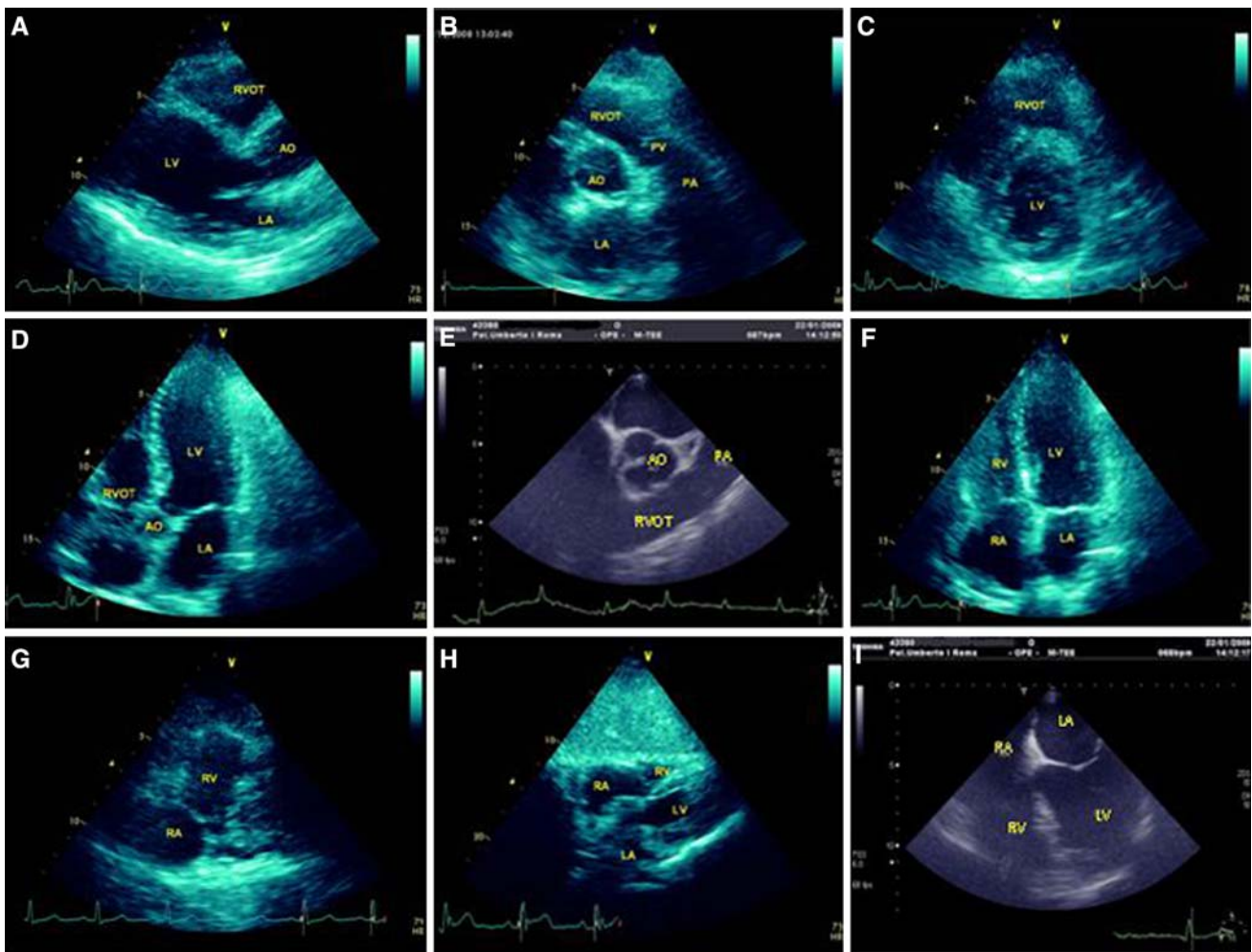


Fig. 2 RV 2D multiple views. *RV outflow*: **a, b, c, d, e**. *RV inflow*: **f, g, h, i**. **a** Parasternal long-axis view. **b** Parasternal short-axis view (great vessels level). **c** Parasternal short-axis view (LV level). **d** Apical long-axis view. **e** Mid-esophageal short-axis view. **f** Apical 4-chamber view. **g** Parasternal RV long-axis view. **h**. Subcostal

4-chamber view. **i** Mid-esophageal 4-chamber view. *Ao* Aorta, *LA* left atrium, *LV* left ventricle, *PA* pulmonary artery, *PV* pulmonary valve, *RA* right atrium, *RV* right ventricle; and *RVOT* right ventricular outflow tract

radionuclide- or MRI-derived RVEF (correlations ranging from 0.65 to 0.80). The most widely used quantitative technique to measure RV ejection fraction (RVEF) is the area-length method in which a traced RV lumen area in the four-chamber view is combined with the RV dimension in the parasternal short-axis view [45, 46].

Right ventricular fractional area change (RVFAC) is a 2D assessment that correlates well with RVEF, determined by volumetric analysis using cardiac MRI and is superior to other 2D methods to assess RV function [48, 49]. Calculation of RVFAC is easily performed on standard echocardiographic equipment and does not require any geometric assumptions. Its simplicity represents its greatest advantage over more complex geometric models of RV function.

The majority of the proposed methods of echocardiographic assessment of RV function are based on volumetric

approximations of the RV. Such approaches have inherent limitations, first as volume-related measures such as EF are load dependent, second because of the complex geometry of the RV. The issue of RV geometry is usually overcome using geometry-independent parameters such as tricuspid annular excursion and the Tei index.

The measurement of the tricuspid annular plane systolic excursion (TAPSE) estimates RV systolic function by measuring the level of systolic excursion of the lateral tricuspid valve annulus toward the apex in the four-chamber view [50]. A significant correlation between the TAPSE and RV ejection fraction as assessed by radionuclide angiography and MRI-derived volumes was shown. The approach appears reproducible and proved to be a strong predictor of prognosis in heart failure. A TAPSE >1.5 cm was consistently observed in the normal population. Although simple to perform, assessments that depend on tricuspid annular

Table 1 RV M-mode/2D dimensions and systo-diastolic indices

RV index	Normal values	Age (years)	Clinical meaning	Ref.
M-mode dimensions				
RV thickness	3.0 ± 0.92 mm	Adults all ages	≥5 mm → RV hypertrophy	[34]
RVED M-mode	24.3 ± 6.7 mm	61 ± 10	>30 mm → pressure/volume overload	[5]
2D Dimensions				
RVOT thickness (5 regions)	2 to 5 mm	19–46 (mean 32)	≥5 mm → RV hypertrophy	[35]
RV mass	33.0 ± 11.0 g/m ²	2 days–17 years	>35 g/m ² → RV hypertrophy	[37]
RVED mid-transverse 4C	2.7–3.3 cm	19–46 (mean 32)	>3.3 cm → pressure/volume overload	[35]
RVED base-to-apex 4C	7.1–7.9 cm	19–46 (mean 32)		[35]
RVEDA	17 ± 3 cm ²	52 ± 20		[47]
RVESA	8 ± 3 cm ²	52 ± 20		[47]
RVEDA/LVEDA	≤2/3		>2/3 → RV myocardial disease	[36]
RVEDA/LVEDA-TEE	0.54 ± 0.12	Adults all ages	>0.6 → dilated RV, > 1 → severe ACP	[38]
RVOT (above aortic valve)	2.5–2.9 cm	19–46 (mean 32)	>3 cm → abnormal	[35]
RVOT-TEE (above aortic valve)	2.7 ± 0.4 cm	20–75(45 ± 16)	>3 cm → abnormal	[39]
Systolic indices				
RVOTFS	61 ± 13%	46 ± 12	Focuses on RVOT function	[44]
RVEF	46 ± 7%	59 ± 16	Clinical validation, wide acceptance	[5]
RVFAC	51 ± 11%	52 ± 20	Good correlation with RVEF	[47]
TAPSE	15–20 mm		Good correlation with RVEF	[50]
RV MPI (Tei Index)	0.32 ± 0.03	3–18	>0.4 → RV dysfunction	[52]
RV stress/velocity (MNSER _c)	1.3 ± 0.19 DV/s	1 day–54 years	Reliable index of contractility	[55]
dP/dt max	100–250 mmHg/s		Not reliable index of contractility	[13]
Maximal RV elastance	1.30 ± 0.84 mmHg/ml		Reliable contractility index (research)	[10]
Diastolic indices				
RV E/A	1.50 ± 0.3	20–86 (57 ± 12)	>2 suggests restriction	[61]
RV DT	198 ± 23 ms	20–86 (57 ± 12)	<160 ms suggests restriction	[61]
IVC	≤1.7 cm, CI ≥ 50%	66 ± 13	Estimates RAP (>2 cm → poor outcome)	[63]
Hepatic vein S/D	>1 in SR, <1 in AF	21–84	Reversal in diastolic dysfunction	[60]
Respiratory variation in E velocity	TV ≤15%insp.↑, MV ≤10%insp.↓	55 ± 15	Ventricular interdependence	[23]
Pressures estimates				
TR peak velocity	2.1 ± 0.4 m/s		>2.5 m/s → PHT	[78]
PA Acc. time	128 ± 13 ms		<100 ms → PHT	[78]

4C 4-chambers view, ACP acute cor pulmonale, AF atrial fibrillation, CI collapsibility index, dP/dt rate of pressure development, DV/s diastolic volume/second, DT deceleration time, E early diastolic, E/A early diastolic/late diastolic, IVC inferior vena cava, LVEDA left ventricular end diastolic area, MNSER_c rate corrected mean normalized systolic ejection rate, MPI myocardial performance index, MV mitral valve, PA pulmonary artery, PHT pulmonary hypertension, RAP right atrial pressure, RV right ventricle, RVED right ventricular end diastolic diameter, RVEDA right ventricular end diastolic area, RVESA right ventricular end systolic area, RVEF right ventricular ejection fraction, RVFAC right ventricular fractional area change, RVOT right ventricular outflow tract, RVOTFS right ventricular outflow tract fractional shortening, S/D systolic/diastolic, SR sinus rhythm, TAPSE tricuspid annular plane systolic excursion, TR tricuspid regurgitation, TV tricuspid valve, and TEE transesophageal echocardiography

excursion have inherent limitations as independent measures of RV systolic function [51].

The Doppler index of myocardial performance (Tei index or MPI-myocardial performance index-) is another nongeometric index of RV global ventricular function [52, 53]. MPI is ratio of sum of isovolumic contraction time (IVCT) and isovolumic relaxation time (IVRT) divided by ejection time (ET): MPI = (IVCT + IVRT)/ET. Increasing value correlates with increasing ventricular dysfunction.

It is established that it is actually unaffected by heart rate, loading conditions or the presence and the severity of tricuspid regurgitation. An MPI of >0.4 has 100% sensitivity and negative predictive value in identifying abnormal RVEF. However, calculation of the parameter is not always feasible. It can be pseudonormalized in the presence of a decrease in isovolumic contraction time associated with an acute increase in RV diastolic pressure as it may happen in severe RV myocardial infarction [54].

In the left ventricle, the relationship between rate corrected mean velocity of circumferential fiber shortening and systolic wall stress has been shown to be independent of heart rate, preload, and afterload. The same concept was used [55] to evaluate the relationship between peak systolic wall stress in RV and mean normalized systolic ejection rate (MNSER) in patients with isolated ASD II (volume overload), pulmonic stenosis (pressure overload), and normal subjects. Over a wide range of loading conditions, it was shown that increases in peak systolic wall stress cause an incremental slowing of MNSER corrected for heart rate. If further studies confirm that this is an independent measure of RV contractility, then it may represent a clinically useful means to distinguish between contractile and pump dysfunction.

The rate of pressure development (dP/dt max) is also used as an index of RV contractility. As demonstrated by numerous studies, RV dP/dt max is significantly affected by loading conditions and cannot be used as a reliable index of contractility [12]. It may, however, be useful in assessing the directional change in response to therapy.

Maximum ventricular elastance (as discussed earlier) is considered by many investigators as the best index of contractility [9], but since it is based on conductance catheterization that is invasive and time consuming, it is predominantly used as a research tool for the assessment of ventricular function.

Continuous wave Doppler is used to estimate pulmonary artery systolic and mean diastolic pressure by measuring the peak retrograde pressure drop across the tricuspid valve (TR) and pulmonary valve, respectively. Peak TR gradient is today the most commonly used method to assess pulmonary artery systolic pressure in clinical practice [56]. Measures that do not depend on RV function, such as pulmonary artery pressure and pulmonary vascular resistance, are poor predictors of survival, even though afterload is the dominant cause of RV failure. It appears that there is a threshold level of afterload beyond which RV response becomes the main determinant of survival and quality of life. Pulmonary artery pressure remains a nodal point, since the primary cause of death in patients with PAH is RV failure caused directly and indirectly by the elevated pulmonary pressures. However, despite its crucial role, pulmonary artery pressure gives us little more information on RV function than systemic pressure tells us about LV function.

As with LV systolic dysfunction, the improvement during exercise confers a better prognosis and effort tolerance. Three-dimensional assessment of RV contractile function is difficult enough at rest, similarly complex measures such as the Tei index are not possible in most patients during exercise. In every day practice, the only available measure during exercise is the tricuspid gradient

[57], and the change in pressure during exercise has not yet been correlated with clinical outcome. Cardiopulmonary exercise testing provides many measures, the VO_2 max in particular correlates well with prognosis and quality of life. In expert hands, this is a reproducible technique, but improved standardization is desirable, since interobserver variability between different centers can give inconsistent results [58].

Right ventricular diastolic function

Conceptually, diastolic suction is that property of the ventricle by which it tends to refill itself during early diastole, independent of any force from the atrium. RV diastolic abnormalities such as reduced myocardial compliance may impair systolic function by limiting filling and play an integral role in cardiac adaptations to disease. Nevertheless, the development of indexes for RV function has evolved slowly, and numerous gaps remain in our understanding of RV diastolic function. New model parameters and related diastolic properties that allow accurate quantitative assessment of RV diastolic function abnormalities in animal models have been described [59].

Pulsed wave Doppler interrogation of the RV inflow (RV E/A ratio), superior vena cava, and hepatic veins has been advocated in the comprehensive evaluation of RV diastolic function [60–62] in various diseases including pericardial tamponade, constrictive pericarditis, restrictive cardiomyopathy, and congenital heart disease. The phase of respiration markedly influences superior vena cava flow, hepatic vein, and RV inflow velocities. During inspiration, with increased venous return, there is a tendency to increase flow velocities, whereas in expiration, there is a tendency to decrease venous flow. The forward systolic and diastolic flow velocities and velocity integrals appear significantly greater than during expiration and apnea, whereas there is greater flow in apnea than in expiration. The percent change with respiration from expiration to inspiration is approximately 20%. These findings emphasize the need for monitoring the phase of respiration in the assessment of RV diastolic filling. However, although the assessment of RV diastolic function is complex, and many factors can influence the variables including depth of respiration and transducer and patient position, the RV flow patterns should include abnormal relaxation and pseudo-normal and restrictive filling. In general, the largest superior vena cava peak atrial reversal should be <20 cm/s, the RV peak E/A ratio should be $>0.8 < 2$, and deceleration time should be between 160 and 240 ms.

An estimation of right atrial pressure can be obtained from measuring the inferior vena cava (IVC) dimensions and its diameter variation during normal breathing

(collapsibility index). A reduction in inferior vena cava (IVC) diameter of more than 50% is consistent with right atrial pressure <10 mmHg [36]. A small IVC (<1.2 cm) with spontaneous collapse is often seen in the presence of intravascular volume depletion. A dilated IVC without collapse with inspiration suggests a markedly increased RA pressure (>15 mmHg) and remains associated with worse survival independent of a history of heart failure, other comorbidities, ventricular function, and pulmonary artery pressure [63].

RV function during acute RV pressure overload consistently showed no significant change in RV diastolic performance, despite a rise in RV elastance. However, chronic RV pressure overload implies RV diastolic dysfunction with prolonged diastolic relaxation times and increased RV diastolic stiffness [64]. Tissue Doppler echocardiography has been used in the assessment of RV diastolic function [65–70]. An *in vitro* study showed that E/E_a , IVRT and the RV Tei index were significantly increased in rats with PH induced by monocrotaline compared with controls [67], and it has been concluded that TDI was more accurate in assessing both RV diastolic and RV global dysfunctions. Furthermore, the RV E/E_a ratio, an indicator of RV filling pressure increase in RV hypertrophic cardiomyopathies, was significantly increased in PH rats. In humans, E/E_a can correct for the influence of relaxation on E and relates strongly to RV filling pressure. A lower cutoff RV E/E_a than that determined to estimate high LV filling pressure is expected, because tricuspid annular velocities are higher, and inflow velocities are lower than the LV filling site. An RV E/E_a ratio >6 suggests a mean RAP >10 mm Hg [68], but we should be cautious to use this index in patients with early after cardiac surgery and in patients with normal RV function [69]. It has also been shown [70] that serum brain natriuretic peptide (BNP) correlates with RA contractility and RV diastolic dysfunction by RV TDI in adults with acquired PH and suggested that increased BNP may be related to decreased RA systolic function and RV diastolic function.

Only a few studies have addressed the prognostic importance of RV diastolic function [62, 71–73]. The difficulty in studying RV diastolic function may be explained by the marked load dependence of RV filling indices. Survival is predicted for patients with idiopathic dilated cardiomyopathy by increased diastolic right ventricular chamber area measured echocardiographically, and survival of patients with right ventricular enlargement out of proportion to left ventricular enlargement is poorer [71]. Survival, left ventricular ejection fraction, and symptoms are worse in dilated cardiomyopathy patients with angiographically documented biventricular dysfunction compared with those with left ventricular dysfunction alone [72]. In patients with left HF, it has been shown [73] that

RV diastolic dysfunction defined by abnormal filling profiles is associated with an increased risk of nonfatal hospital admissions for HF or unstable angina.

Three-dimensional echocardiography

The clinical use of three-dimensional echocardiography has been neglected due to the prolonged nature of data acquisition. The recent introduction of real-time three-dimensional echocardiography (RT3DE) implied a great progress in echocardiography as images may be obtained in just one beat. This has been accomplished with a full matrix array transducer and improved image resolution, higher penetration and harmonic capabilities, usable for both gray scale and contrast imaging. Moreover, this transducer displays “on-line” three-dimensional volume-rendered images and is capable of displaying two simultaneous orthogonal two-dimensional imaging planes. The major advantage of RT3DE is that volumetric analysis does not rely on geometric assumptions, as is the case with 2D echocardiography. Quantitation of LV volumes and mass using RT3DE has been performed successfully from an apical wide angled acquisition using different methods. A similar approach can be applied for RV evaluation [74–76]. Data analysis may be performed online or offline with dedicated three-dimensional software (TomTec GMBH, Munich, Germany), and multiple slices may be obtained from the base to the apex of the heart as in the method of discs.

Three-dimensional imaging combined with analysis using the multiple slice technique is more accurate, because reliance on geometric modeling is eliminated. The contours of the RV endocardium are delineated in parallel planes, the area of each “slice” is multiplied by the slice thickness to compute slice volume, and the volumes of the slices are summed to compute RV volume. RV quantitation by 3D echo is not only performed in short-axis slices; the same software package will also perform long axis tracings in any number of slices (e.g. 8), in essence providing an 8-plane Simpson’s method for quantitation. Additionally, newer software released from the same company will perform semi-automated 3D border tracking rather than being limited to 2D slices through a 3D structure. These methods may potentially make 3D echo more accurate.

Three-dimensional echocardiography is a promising new method for calculating RV volumes and EF (Table 2), comparing well with MRI-derived values and, in particular, correlating very closely with RV EF calculated by radionuclide techniques. The accuracy of TTE-3D was comparable to that of TEE-3D [74]. Boundary tracing error remains the largest source of error. Variable visualization of the apex can be minimized by carefully manipulating the

Table 2 RV three-dimensional and myocardial imaging indices

RV index	Normal values	Age (years)	Clinical meaning	Ref.
3D indices				
3DRVEDV	70.97 ± 15.06 ml	39 ± 22	>100 ml → volume overload	[75]
3DRVESV	39.88 ± 10.46 ml			[75]
3DRVEF	44 ± 7%			[75]
3DRVEF-TEE	34–62	23–76	Good correlation with 3DRVEF-TTE	[74]
Myocardial imaging indices				
RV S_a	15.5 ± 2.6 cm/s	17–63 (49 ± 11)	<11.5 cm/s → RV dysfunction (RVEF <45%)	[79]
RV E/E_a	<6	36–90 (68 ± 10)	Estimates RVEDP (>6 → RAP ≥ 10 mmHg)	[68]
RV IVA	1.8 ± 0.6 m/s ²	8–41 (21 ± 14)	Reliable index of contractility (CHD)	[88]
RV IVRT/RR	<10%	23–75 (52 ± 12)	>10% → PASP >30 mmHg	[91]
RV strain	Basal −21 ± 6.6%	Adults all ages	Correlates with stroke volume	[111]
	Mid −27 ± 9.9%			[111]
	Apical −28.7 ± 9.9%			[111]
	All segments −25.4 ± 9.5%			[111]
RV strain rate (all segments)	S −1.56 ± 0.61 s ^{−1}		Correlates with contractility	[111]
	E −2.39 ± 1.15 s ^{−1}			[111]
	A −1.24 ± 0.69 s ^{−1}			[111]
RV 2D-strain	Basal −22.6 ± 7.4%		Correlates with stroke volume	[111]
	Mid −24.4 ± 7.7%			[111]
	Apical −27.6 ± 8.9%			[111]
	All segments −24.8 ± 8.2%			[111]
RV 2D-strain rate (all segments)	S −1.45 ± 0.53 s ^{−1}		Correlates with contractility	[111]
	E −1.85 ± 0.80 s ^{−1}			[111]
	A −1.10 ± 0.49 s ^{−1}			[111]

3DRVEDV 3-dimensional right ventricular end diastolic volume, *3DRVESV* 3-dimensional right ventricular end systolic volume, *3DRVEF* 3-dimensional right ventricular ejection fraction, *3DRVEF-TTE* 3-dimensional right ventricular ejection fraction-transesophageal echocardiography, *3DRVEF-TTE* 3-dimensional right ventricular ejection fraction-transthoracic echocardiography, *A* atrial (late diastolic), *CHD* congenital heart disease, *E* early diastolic, *PASP* pulmonary arterial systolic pressure, *RAP* right atrial pressure, *RV E/E_a* tricuspid early diastolic flow velocity/early diastolic annular velocity ratio, *RVEDP* right ventricular end diastolic pressure, *RVEF* right ventricular ejection fraction, *RV IVA* RV myocardial acceleration during isovolumic contraction, *RV IVRT/RR* RV isovolumic relaxation time corrected for heart rate, *RV S_a* tricuspid annular systolic velocity, *S* systolic

entire 3D data set, so that the largest long axis is visualized and prescribing a series of short-axis images such that they are perpendicular to the long axis. Errors with 3D echo arrive also from the fact that it is difficult to acquire a 3D dataset of the RV including the RVOT, as this is a very anterior structure, often obscured by near-field artefacts. Future developments in automatic image segmentation, possibly with the help of contrast agents, may improve results. This task is more difficult for the RV than for the LV due to the RV's heavy trabeculation, prominent intraventricular structures, and complex shape.

What is known concerning the 3D pattern of RV regional function comes from MRI tagging in which the heart's magnetization is locally perturbed in order to create a visible marker whose motion reflects that of the underlying myocardium. Tagging studies have documented the heterogeneity of normal RV wall motion, confirmed greater long axis than short-axis shortening, quantified torsion, and

provided detailed analysis of the motion of the RV free wall toward the interventricular septum. However, there is no consensus on how regional wall motion should be assessed. For the LV, the standardized 16 or 17 segment model into which the standard LV views are divided have correspondence to coronary artery territories. However, no segmentation plan was presented for the RV in the "Recommendations for chamber quantitation" recently published by the American and European Societies of Echocardiography [36].

Myocardial imaging echocardiography

Tissue Doppler imaging (TDI)

TDI allows quantitative the assessment of RV systolic and diastolic function (Table 2) by means of measurement of

myocardial velocities [77, 78]. In contrast to conventional color flow Doppler echocardiography, which detects high velocity with low amplitudes, TDI detects low velocity with high amplitudes. The earlier studies used pulsed-wave TDI to examine RV function. Two-dimensional color-coded TDI allows true offline analysis of multiple segments simultaneously (Fig. 3). However, it provides mean values compared to pulsed TDI that provides peak velocities and has lower temporal resolution, although a frame rate above 100 frames per second is considered acceptable. A systolic annular velocity $<11.5 \text{ cm s}^{-1}$ predicted right ventricular dysfunction (ejection fraction $<45\%$) with a sensitivity of 90% and a specificity of 85% [79]. RV peak systolic velocity impairment has been observed in patients with scleroderma, obstructive sleep apnea syndrome, and LV failure [80–84]. Moreover, noninvasive estimation of right atrial pressure is possible [67, 69] using trans-tricuspid

pulsed-wave Doppler and TDI (E/E_a). However, clinical experience in patients is limited, and further studies with TDI assessing RV function are being pursued.

TDI has also been used to determine systolic and diastolic time intervals and myocardial performance index (Tei index). Although the isovolumic phases of IVCT and IVRT are slightly longer when measured by TDI versus pulsed Doppler, it has been shown that TDI-determined Tei index (Fig. 3a) correlates well with the Tei index determined by flow Doppler, and thus represents a simple method of assessing RV myocardial performance with the advantage of simultaneous recording of systolic and diastolic velocity patterns [85, 86].

The myocardial acceleration during isovolumic contraction (IVA) represents a new tissue Doppler-derived parameter of systolic performance. It is calculated by dividing the maximal isovolumic myocardial velocity by

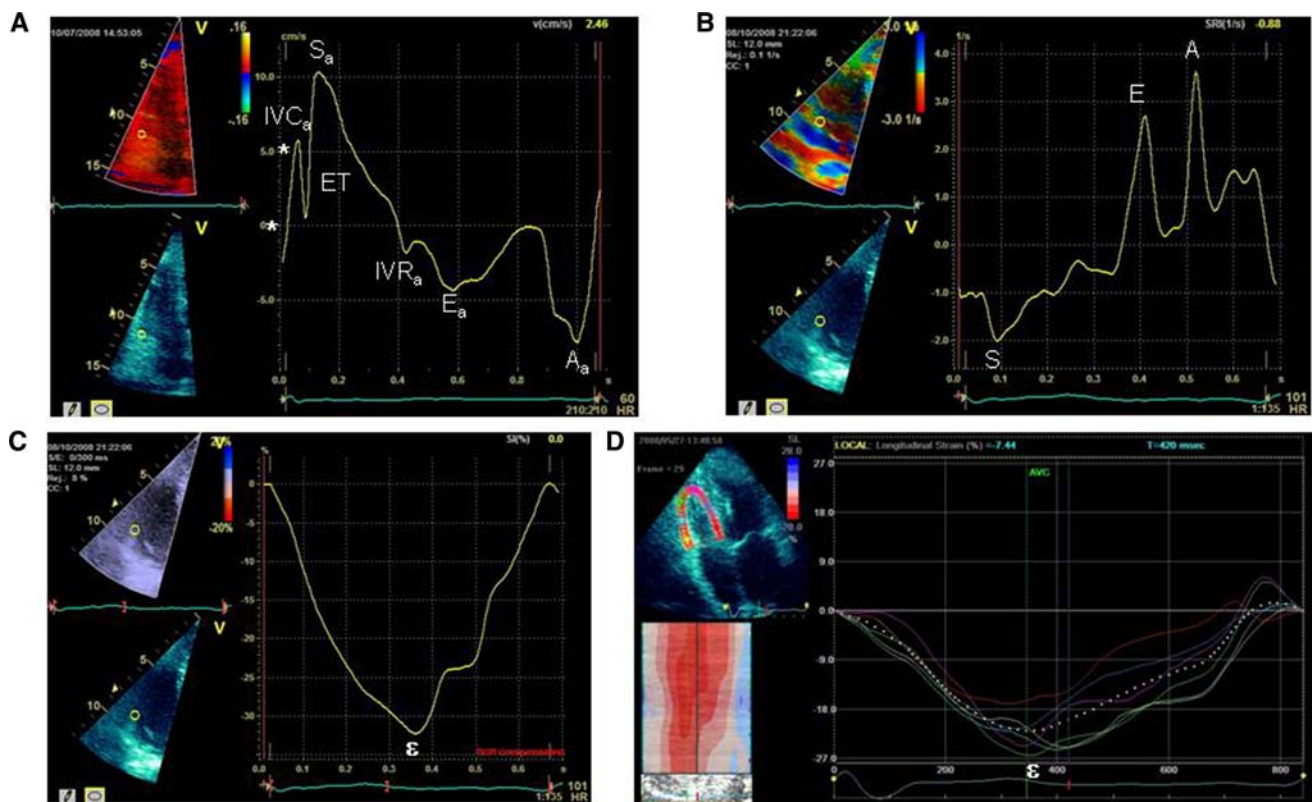


Fig. 3 RV TDI and STI tracings in normal subjects. **a** TDI velocity tracing at tricuspid annulus site. Peak systolic velocity at annulus level (S_a), isovolumic contraction peak positive velocity (IVC_a), isovolumic relaxation peak negative velocity (IVR_a), peak early diastolic velocity (E_a), peak late atrial velocity (A_a), and ejection time (time difference between onset to end of ejection, ET) are shown. The isovolumic myocardial acceleration (IVA) is calculated as the difference between baseline and peak velocity (*stars*) during isovolumic contraction divided by their time interval. The isovolumic contraction time (IVCT) is measured as the time difference between the end of A_a to the onset of S_a , the isovolumic relaxation time (IVRT) is measured as the time difference between the end of ejection

to the onset of E_a . The MPI (myocardial performance index) is calculated as $(IVCT + IVRT)/ET$ (see text). **b** 1D-strain rate (SR). Systolic (S), early diastolic (E), and late diastolic (A) SR values are shown. **c** 1D-strain. Representative example of a strain curve. ϵ = peak systolic strain (peak of maximal deformation). **d** 2D-strain. A 6-segment model of the right ventricle is created by the tracking algorithm after manual delineation of the endocardial border. The onset of QRS signifies the zero deformation point. The global (*dotted line*) and segmental (*colored lines*) strain curves represent the relative (percentage) shortening of the region of interest as a function of time. ϵ = peak systolic strain

the time to peak velocity: IVA = maximum velocity/time to peak (Fig. 3a). The value of myocardial IVA has been studied [87] in a closed-chest animal model during the modulation of preload, afterload, contractility, and heart rate, and it has been showed that IVA reflects RV myocardial contractile function and is less affected by preload and afterload within a physiological range than either the maximum first derivative of RV pressure development (dP/dt max) or ventricular elastance. Clinical studies confirmed its value in congenital heart disease, after repair of tetralogy of Fallot and in transposition of the great arteries [88, 89]. Further validation of this new index is warranted. However, it has been shown that modern echocardiographic estimates of RV contractility and function, such as tricuspid annular plane systolic excursion, IVA, and regional myocardial velocity by TDI, are stable with moderate changes in preload and afterload in healthy individuals with the exception of the Doppler-derived index of myocardial performance, which proved less stable with increased afterload [90].

By the use of TDI technique, it has been confirmed the known relationship between isovolumic relaxation time (IVRT) and pulmonary artery systolic pressure (PASP). It has been shown that TDI-derived IVRT corrected for heart rate correlates well with PASP, and this method has been proposed as an additional noninvasive tool in the assessment of PASP [91].

Segmental RV dysfunction has been described in patients with RV myocardial infarction [92]. The pattern of regional dysfunction depends on the culprit artery. With the involvement of the right coronary artery proximal to the marginal branches (in a right-dominant coronary system), segmental hypokinesia is seen in the lateral and inferior wall. With the involvement of the posterior descending artery, hypokinesia is usually limited to the inferior segments. In anterior myocardial infarction involving the left anterior descending coronary artery, RV hypokinesia is usually limited to the anterior wall.

TDI allows also the assessment of ventricular dyssynchrony. The study of RV resynchronization is at its initial stages. Although dyssynchrony has been demonstrated in the LV, the prevalence and hemodynamic consequences of RV dyssynchrony in cardiac disease are not well defined. RV dyssynchrony may affect the coordination of contraction in different RV regions resulting in reduced cardiac output, but this phenomenon may also be mediated by the change in movement of the interventricular septum. Resynchronization of the failing RV may be divided into 2 categories: resynchronization of the systemic RV and resynchronization of the pulmonic RV. Even if the number of RV segments that can be assessed by TDI is limited, the measurement of septum-to-RV free wall dyssynchrony is feasible (Fig. 4). In heart failure patients with a prolonged

QRS duration on the ECG, septum-to-RV free wall dyssynchrony has been observed, which was reversed after cardiac resynchronization therapy. A multicenter international study demonstrated that cardiac resynchronization therapy was associated with improvement in RVEF in patients with either systemic or pulmonic RV [93]. RV dyssynchrony has been suggested to predict response to cardiac resynchronization therapy [94–96], but other studies should confirm these preliminary observations. Also, it is not clear whether patients with isolated RV dyssynchrony will benefit from cardiac resynchronization therapy, and future studies are desirable to understand the clinical meaning of this dyssynchrony.

Strain rate imaging (SRI or 1D-strain)

Strain is defined as the degree of deformation of an object, whereas, strain rate represents the speed at which strain occurs [97]. In mathematical models and in experimental studies, longitudinal strain appears to correlate best with changes in stroke volume, whereas, longitudinal strain rate is more related to local contractile function and appears to be more independent of loading. The assessment of RV longitudinal strain from the apical views (Figs. 3, 4) is feasible in the clinical setting [98–100]. In normal subjects, RV longitudinal velocities show a baso-apical gradient with higher velocities at the base and appeared consistently higher when compared to the LV [98]. This can be explained by the differences in loading conditions and compliance with a lower afterload in the RV and by the dominance of longitudinal and oblique myocardial fibers in the RV free wall. Moreover, compared to the LV homogeneous distribution of deformation properties, RV strain rate and strain values have an inhomogeneous distribution and show a reverse baso-apical gradient, with the highest values in the apical and outflow areas. The inhomogeneous distribution of regional wall stress can be related to the complex geometry of the thin-walled crescent-shaped RV compared to the thick-walled bullet-shaped LV.

Interestingly, in the systemic RV [100], it has been reported a shift in the ventricular free wall from longitudinal to circumferential shortening when compared with the normal RV but without any change in septal shortening. The systemic RV is more similar to the normal LV, which has a well-developed middle circumferential layer. The leftward septal shift with decreased radius of curvature gives the systemic RV a more circular short-axis shape facilitating circumferential shortening through reduced regional wall stress. Thus, the systemic RV contraction pattern resembles that of the normal LV, but without the ventricular torsion of its normal systemic counterpart. Since strain values were similar to those in the normal LV, the shortening pattern with predominant circumferential

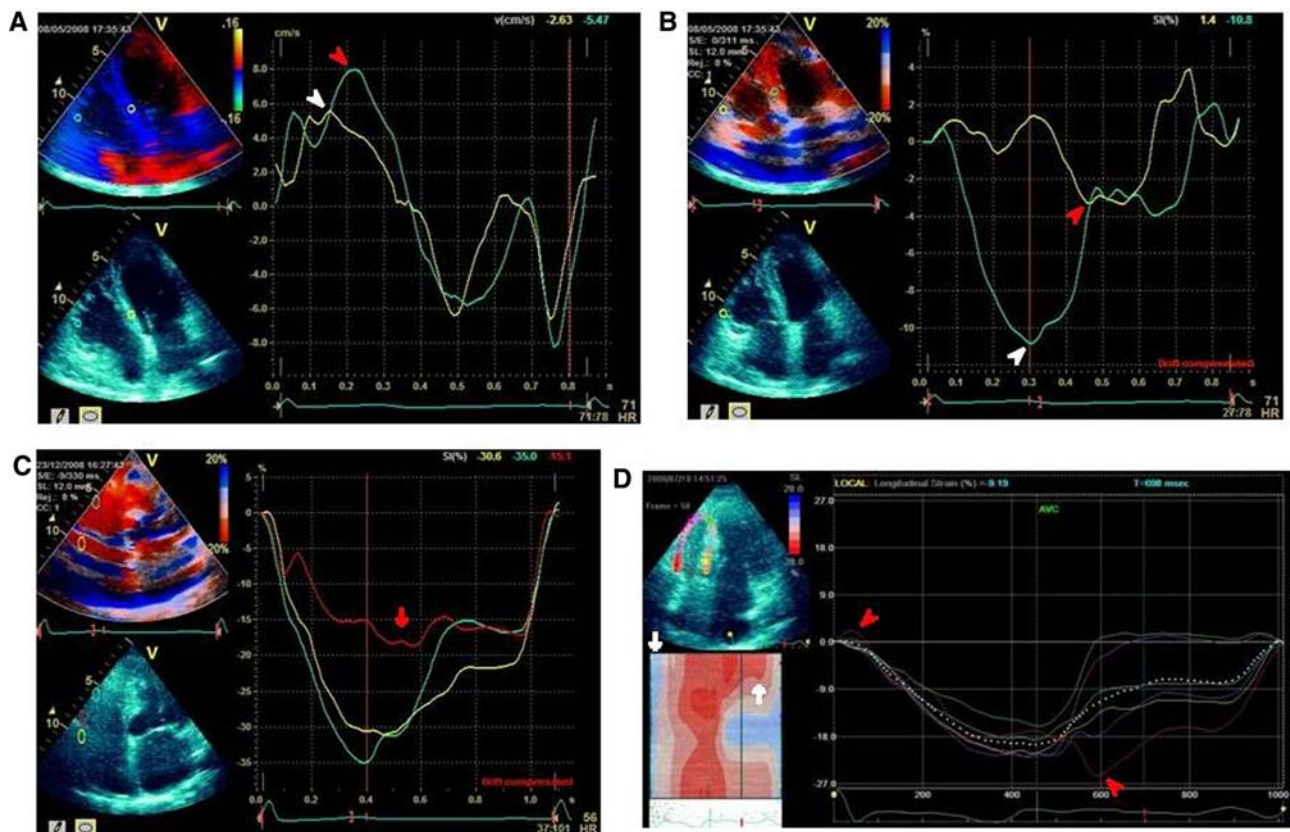


Fig. 4 RV TDI and STI tracings in patients with RV disease. **a, b** RV dyssynchrony in chronic pulmonary hypertension. Delayed time to peak longitudinal peak systolic velocity (A) and strain (B) of the right ventricular free wall (red arrows) compared to the septum (white arrows) in a heart failure patient with pulmonary hypertension. **c** Acute cor pulmonale (pulmonary embolism). Strain curves of apical (green), middle (red), and basal (yellow) part of RV free wall in apical 4-chamber view. The midpart of RV free wall (red arrow) has low strain, whereas, these changes are not seen in the apical and basal

over longitudinal free wall contraction could represent an adaptive response to the systemic load. The absence of basal and apical rotation and torsion and reduced strain rate could imply less energy-efficient ejection and a potential for myocardial dysfunction. Future three-dimensional studies could provide further insights into the deformation of the systemic RV.

Doppler-derived strain measurements (Table 2) have been shown to correlate well with sonomicrometry segment length measurements both in the inflow and outflow tract of the RV and under different loading conditions [101]. Experimental data also showed that regionally derived isovolumic indices of myocardial tissue deformation correspond to the global contractile state of the RV and appear to be less sensitive to increased afterload conditions compared to ejection-phase indices [102].

Changes in regional RV myocardial function after bilateral lung transplantation have been reported in a patient with primary pulmonary hypertension [103]. Conventional

echocardiography showed a significant improvement in RV size and global function after successful transplantation, but strain rate imaging revealed that the functional improvement was limited to the apical trabecularized portion of the RV, and that the smooth inlet segment did not improve after afterload reduction.

Other findings have been reported in chronic and acute settings. The available experience on strain rate imaging for the assessment of regional RV function in chronic pulmonary hypertension is limited to single center studies [104, 105]. It seems that regional analysis of myocardial function may enable the early diagnosis of imminent RV failure before irreversible damage will occur. As a result of their different muscular arrangements, each of the three RV morphologically distinct units could respond differently to both changes in preload and afterload and fiber stretch as a result of dilatation. This could explain the nonhomogeneous decrease in systolic deformation that occurs in patients with chronic obstructive pulmonary disease during times of

worsening hypoxia, and hence increased afterload stress. The technique seems feasible for the quantitative assessment of RV function and may improve understanding of the pathophysiology of different diseases, but the clinical value has not yet been proven in large controlled studies.

Distinct patterns of segmental RV dysfunction have been reported in acute pulmonary embolism (normally contracting right ventricular apex associated to a severe hypokinesia of the mid-free wall -"McConnell sign"-) and RV myocardial infarction [106]. These patterns represent only indirect measures of RV function. In patients with submassive pulmonary embolism and moderate systolic failure, a strain pattern [107] has been described demonstrating the failure of the midpart of the RV free wall. The midpart of RV free wall initially had low or even positive strain, which gradually normalized during the period of observation after thrombolysis. These changes were not seen in the apical and basal segments. The findings were in concordance with the McConnell sign in pulmonary embolism.

Two-dimensional strain (2D-strain) echocardiography or speckle tracking imaging (STI)

Ultrasound tissue deformation imaging has been shown to be an interesting new approach for the assessment of regional myocardial function. However, the angle dependence of the currently available TDI techniques makes its clinical applicability more difficult. For RV functional assessment in patients with PAH and dilated right ventricles, this is an even more severe problem because of the limited number of acoustic windows through the human thorax. To overcome this problem, a new method that also allows the simultaneous estimation of radial and longitudinal strain has been reported recently [108, 109].

Speckle tracking is an application of pattern matching technology to ultrasound cine data. A square template image is created using a local myocardial region of the starting frame of the image data. Multiple templates can be used to observe the movement of the entire myocardium. The process is then repeated by creating new templates and observing their movement in the subsequent frames until the entire cardiac cycle has been assessed. Myocardial deformation is calculated from continuous frame-by-frame tracking of speckled myocardial patterns generated by irregularities in acoustic backscatter. This method does not make use of Doppler information, so there is no Doppler angle dependency.

Longitudinal shortening of the RV has been shown to be a more important contributor to the RV systolic function compared with circumferential shortening [77]. Therefore, longitudinal strain and SR measurements reflect regional RV function, and these parameters could serve as useful

tools for quantitative evaluation (Figs. 3, 4; Table 2). 2D strain echocardiography (STI) has been validated in the LV with sonomicrometry and magnetic resonance imaging tagging *in vitro* and *in vivo*, and new clinical applications of this technique on LV and RV function [110–116] are currently being explored.

It has been suggested that the use of systolic indices derived from color TDI and 2-D strain echocardiography can be proposed as an adjunctive tool in the comprehensive evaluation of RV function in patients with PAH at baseline and after chronic vasodilator therapy. A recent study [111] directly compared TDI and STI measurements in the RV in a head-to-head fashion. It has been shown a good and comparable feasibility for both techniques, and a comparable interobserver and intraobserver reproducibility. Both techniques showed comparable values with similar capacity to distinguish between different pathophysiologic conditions. Only a small bias toward higher values in TDI-derived strain and SR was observed. The overall correlation between the two techniques was moderate to good for strain and SR values. Altered RV geometry had no impact on the comparability of both techniques. Nevertheless, the relatively large limit of agreement for repeated measurements found for both TDI and STI still constitutes a practical limitation to reliable depiction of subtle changes in RV function in the assessment and follow-up of the individual patient.

A recent study on speckle tracking imaging [112] showed clear differences in apical rotational function of the two ventricles, probably based on the underlying myocardial fiber architecture. While the LV in systole rotates in a counterclockwise direction, the RV segments are brought together toward the inferoseptal region, thus inducing a tightening-belt mechanism for reducing its cavity circumference. The results of this study highlight that the LV apical segments rotate uniformly throughout systole, with clockwise rotation during isovolumic contraction and counterclockwise rotation during ejection, as previously described. The RV free wall segments move toward the septum during systole, and this generates different rotational directions of the segments of the free wall. These indices should be examined in a larger group of patients to assess the effect of age and pathologies on rotational function of the two ventricles.

Three-dimensional myocardial imaging echocardiography

Two-dimensional (2D) speckle tracking has the advantage of being unaffected by the incident beam angle when characterizing ventricular mechanical dyssynchrony, whereas tissue Doppler methods are affected by the incident beam angle. However, both techniques are limited to 2D analysis.

To overcome this limitations, triplane tissue Doppler imaging and three-dimensional speckle tracking have been developed [117–120]. Both methods will certainly contribute to the further development of 3D cardiac strain imaging.

A 3D probe allowing simultaneous acquisition of TDI data in three imaging planes is available [120, 121], and a triplane dataset can be obtained. A 3D LV volume can be generated, and LV volumes and ejection fraction calculated. It has been shown that LV dyssynchrony, derived from the triplane-TDI dataset, is predictive for clinical response and LV reverse remodeling after 6 months of cardiac resynchronization therapy [117]. The same principles could be applied to the RV study (Fig. 5a, b).

Speckle tracking is not only limited by its 2-dimensional nature; in a significant proportion of images, there is through-plane motion, leading to de-correlation as the “fingerprint” of 2D speckles that was being tracked is no longer within the image. 3D speckle tracking overcomes this limitation at the expense of primarily temporal resolution, as spatial resolution in 2D is also sacrificed for temporal resolution. In three-dimensional (3D) speckle

tracking [119, 120], instead of using 2D templates to view 2D movement, cubic templates allow to estimate myocardial motion and deformation in three dimensions (Fig. 5b, c). However, the increased field of view of the 3-D ultrasound system typically comes at the expense of both spatial and temporal resolution of the data sets. As a consequence, de-correlation between subsequent ultrasound volumes might become significant. As some methods assume that the gray values or the gray scale patterns of each anatomical structure are relatively constant between subsequent image frames, their application becomes problematic if gray scale patterns differ largely. Solutions to this problem have been approached [120].

Therapeutic implications

The pathophysiologic and echocardiographic concepts we have outlined entail a therapeutic approach to the patient, thus involve both echocardiologists and respiratory physicians. Standard and novel echocardiographic methods of

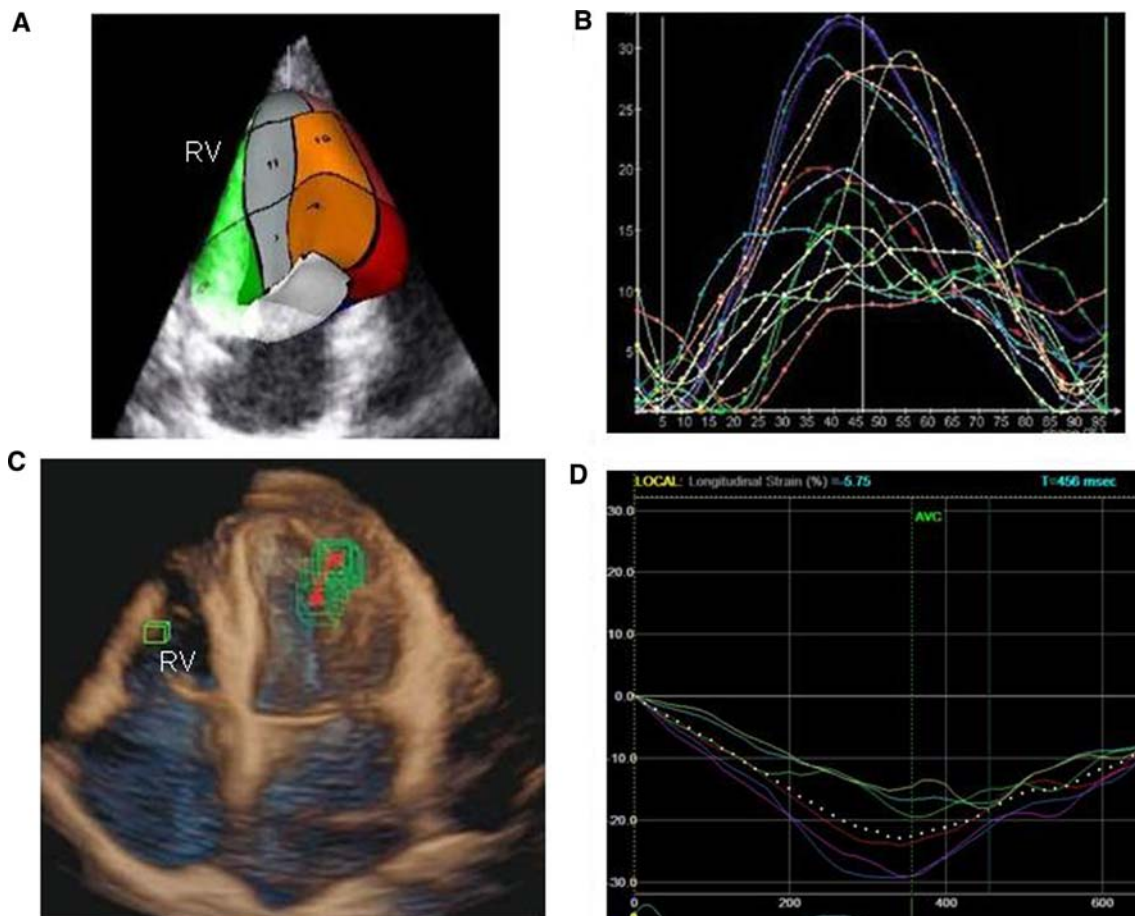


Fig. 5 RV triplane-TDI and 3D-STI. **a** RV 3D reconstruction. **b** TDI tracings from a triplane dataset. **c** Cubic templates. Instead of using 2D templates to view 2D movement, cubic templates allow motion analysis of the ventricles in 3D. **d** STI tracings as 3D tracking result

assessment of RV size and performance contribute to a better understanding of the peculiar chamber-related functional mechanisms in the context of ventricular interdependence and can help clinicians in the treatment of acute and chronic RV failure (Fig. 6). Advances in understanding myocardial mechanics have suggested that clinical application of research in this area may benefit patients in the detection of subclinical disease and tracking changes in disease progression or in response to therapies.

The management of acute and 4-stages chronic RV failure should always take into account the origin of and setting in which RV failure occurs as well as the pathophysiologic aspects. In acute RV failure, every effort should be made to avoid hypotension, which may lead to a vicious cycle of RV ischemia and further hypotension. Specific treatment goals include optimization of preload, afterload, and contractility. Ventricular interdependence also is an important concept to consider when tailoring therapy. The evidence that guides the management of chronic isolated RV failure is not as well established as the evidence that guides the management of chronic HF resulting from LV systolic dysfunction.

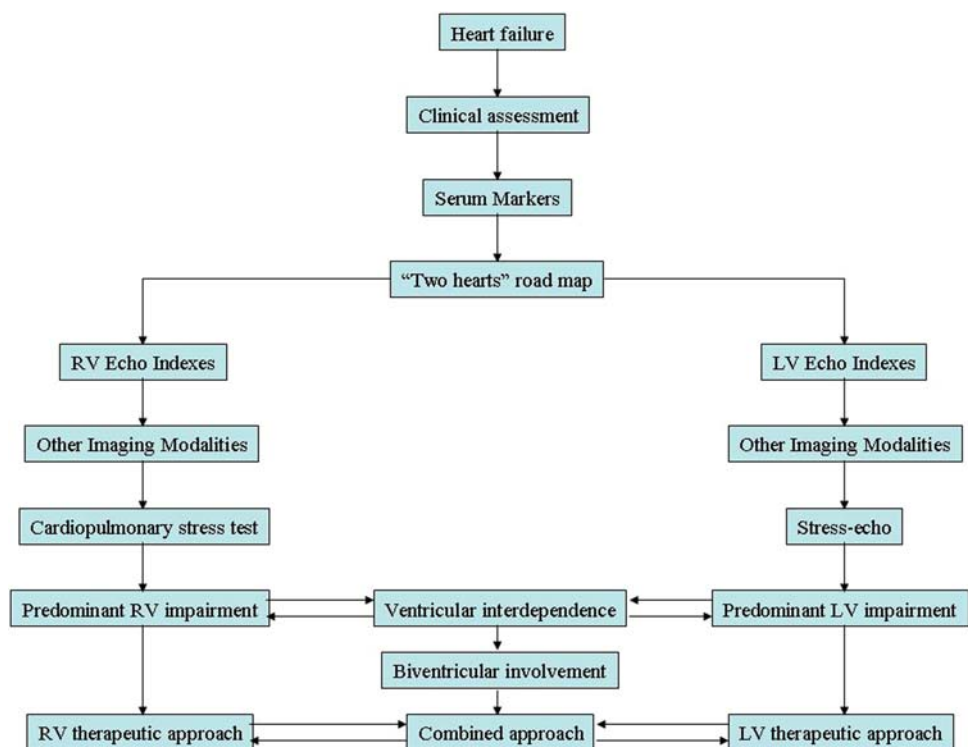
Therapies with inotropes, diuretics, afterload-reducing agents, and β -receptor antagonists have improved the functional status and prognosis of patients with LV failure, but the specific myocardial effects of these therapies for RV dysfunction remain incompletely understood.

In patients with biventricular failure, angiotensin-converting enzyme inhibition has increased RVEF and reduced RV end-diastolic volume and filling pressures [121]. β -blockade with carvedilol or bisoprolol has been shown to improve RV systolic function [122]. Clinical studies assessing the role of angiotensin-converting enzyme inhibitors or angiotensin receptor blockers in the systemic RV have not demonstrated improvement in exercise capacity or hemodynamics, although the studies may have been underpowered [123]. At the present time, the role of β -blockade in RV failure is unclear. In portopulmonary hypertension, β -blockade was associated with worsened exercise capacity and PAH [124].

Digoxin therapy for RV failure has been studied in PAH and chronic pulmonary disease. In PAH, it has been shown that digoxin given acutely may improve cardiac output by approximately 10% [125], but long-term studies are needed to better define its role. In COPD, digoxin therapy did not improve maximal oxygen consumption or exercise or RVEF in patients without LV dysfunction [126].

In patients with acute hemodynamically compromising RV failure, inotropic or vasopressor support may be required. Dobutamine is the most commonly used inotrope in RV failure. In RV myocardial infarction, dobutamine increases the cardiac index and stroke volume, while maintaining preload, and the combination of dobutamine and nitric oxide also has been shown to be beneficial [127]. Levosimendan seems to offer more beneficial effects

Fig. 6 Algorithm for the diagnostic assessment of RV–LV failure



compared to dobutamine in a specific group of patients with biventricular failure and improve ventriculovascular coupling of RV along with the dual benefit of pulmonary vasodilatation and improved RV systolic function [128].

Supplemental oxygen is recommended in patients with evidence of resting or exercise-induced hypoxemia. In patients with RV failure who require ventilatory support, every effort should be made to avoid intrinsic positive end-expiratory pressures, inspiratory pressures >30 mm Hg, permissive hypercapnia, acidosis, and alveolar hypoxia [129]. Evaluation of right ventricular function by transesophageal echocardiography (TEE) in patients with ARDS submitted to protective ventilation revealed the persistence of a 25% incidence of acute cor pulmonale, resulting in detrimental hemodynamic consequences [130]. Patients with hypoxemia associated with TEE-confirmed pulmonary-to-systemic shunting usually do not benefit from supplemental oxygen therapy.

Therapies directed toward pulmonary vasoconstriction and thrombotic factors have improved survival in many patients with severe pulmonary arterial hypertension or pulmonary embolism. Furthermore, acute responsiveness to pulmonary vasodilators is associated with a better prognosis in patients with advanced heart failure [131]. Echocardiographic indices such as two-dimensional strain, myocardial acceleration during isovolumic contraction, and strain rate may complement the current parameters for the assessment of RV systolic function in patients with PAH [131]. However, afterload reduction cannot be obtained in many cases, and the increased RV wall thickness and reversal of a fetal gene expression program have not been investigated as potential targeted treatments.

Both bosentan (endothelin receptor antagonist) and chronic intravenous prostacyclin (epoprostenol) infusion therapy have demonstrated similar improvements in RV function [132–135] in patients with pulmonary arterial hypertension even though the RV dilatation and hypertrophy may not reverse. However, RV function, RV–LV interaction, and RV–pulmonary arterial coupling have been overlooked as potential targets for investigation in regard to therapy.

Intravenous epoprostenol infusion therapy improves survival in idiopathic pulmonary arterial hypertension patients more than in patients with the variant of scleroderma-associated pulmonary arterial hypertension. One possible explanation for this discrepancy in treatment may be the presence of a diffuse myocardial microangiopathy in patients with scleroderma as demonstrated by the impairment of RV functional parameters [80, 136].

Distinctions between the ventricles need to be further evaluated and clarified in animal and human studies to understand the differences, similarities, and interplay between the left and right heart. New therapeutic strategies

for right-heart failure should be investigated including new combinations of existing drugs or new cell-based drugs.

Also, the operative techniques in procedures that try to restore septal architecture after RV dysfunction following RV outflow tract (RVOT) obstruction and RV dysplasia [137–139] aim to rebuild a normal oblique septal anatomic fiber orientation. It has been reported that RV restoration is a safe, simple, and effective surgical procedure that should be added during PVI in patients with severe RV dilatation and aneurysmal/akinetic RVOT, and it has been stressed the concept that a “valve-ventricle” approach rather than the current “valve only approach” is needed in dilated RV failure from the vantage point of geometric correction of RV failure [139].

In conclusion, right and left heart are interdependent and work in synergy, but they are also independent as they are genetically, embryologically, and pathophysiologically different. These differences are corroborated by conventional echocardiography and myocardial imaging echocardiography. The latter modality is not routinely practiced but provides relevant information on regional changes in RV function and adds to the understanding how the differing structural RV components deteriorate after increasing afterload. Thus, in spite of ventricular–ventricular interaction, the “two hearts” concept is a clinically useful mental “road map” because of medical and surgical therapeutic implications. Whereas some RV indices are at the forefront of a new area of clinical research, others yet belong to clinical tools.

References

1. Goor DA, Lillehei CW (1975) Congenital malformations of the heart, 1st edn. Grune and Stratton, New York, pp 1–37
2. Ho SY, Nihoyannopoulos P (2006) Anatomy, echocardiography, and normal right ventricular dimensions. *Heart* 92(1):i2–i13
3. Sheehan F, Redington A (2008) The right ventricle: anatomy, physiology and clinical imaging. *Heart* 94:1510–1515
4. Bleeker GB, Steendijk P, Holman ER, Yu CM, Breithardt OA, Kaandorp TAM, Schalij MJ, van der Wall EE, Nihoyannopoulos P, Bax JJ (2006) Assessing right ventricular function: the role of echocardiography and complementary technologies. *Heart* 92(1): i19–i26
5. Lindqvist P, Calcuttea A, Henein M (2008) Echocardiography in the assessment of right heart function. *Eur J Echocardiogr* 9:225–234
6. Redington AN, Gray HH, Hodson ME, Rigby ML, Oldershaw PJ (1988) Characterisation of the normal right ventricular pressure-volume relation by biplane angiography and simultaneous micromanometer pressure measurements. *Br Heart J* 59: 23–30
7. Dickstein ML, Yano O, Spotnitz HM, Burkhoff D (1995) Assessment of right ventricular contractile state with the conductance catheter technique in the pig. *Circulation* 29:820–826
8. Burger W, Jockwig B, Gerta Rucker G, Kober G (2001) Influence of right ventricular pre- and afterload on right ventricular

- ejection fraction and preload recruitable stroke work relation. *Clin Physiol* 21:85–92
9. Suga H, Sagawa K, Shoukas AA (1973) Load independence of the instantaneous pressure-volume ratio of the canine left ventricle and effects of epinephrine and heart rate on the ratio. *Circ Res* 32:314–322
 10. Dell'Italia LJ, Walsh RA (1988) Application of a time varying elastance model to right ventricular performance in man. *Cardiovasc Res* 22:864–874
 11. Kass DA, Maughan WL (1988) From “Emax” to pressure-volume relations: a broader view. *Circulation* 77:1203–1212
 12. Goldstein JA (2002) Pathophysiology and management of right heart ischemia. *J Am Coll Cardiol* 40:841–853
 13. Haddad F, Hunt SA, Rosenthal DN, Murphy DJ (2008) Right ventricular function in cardiovascular disease, part I—atomy, physiology, aging, and functional assessment of the right ventricle. *Circulation* 117:1436–1448
 14. Diller GP, Dimopoulos K, Kafka H, Ho SY, Gatzoulis MA (2007) Model of chronic adaptation: right ventricular function in Eisenmenger syndrome. *Eur Heart J Suppl* 9:H54–H60
 15. Beghetti M, Galiè N (2009) Eisenmenger syndrome: a clinical perspective in a new therapeutic era of pulmonary arterial hypertension. *J Am Coll Cardiol* 53:733–740
 16. Haddad F, Doyle R, Murphy DJ, Hunt SA (2008) Right ventricular function in cardiovascular disease, part II—pathophysiology, clinical importance, and management of right ventricular failure. *Circulation* 117:1717–1731
 17. Voelkel NF, Quaife RA, Leinwand LA, Barst RJ, McGoon MD, Meldrum DR, Dupuis J, Long CS, Rubin LJ, Smart FW, Suzuki YJ, Gladwin M, Denholm EM, Gail DB (2006) Right ventricular function and failure: report of a national heart, lung, and blood institute working group on cellular and molecular mechanisms of right heart failure. *Circulation* 114:1883–1891
 18. Bogaard HJ, Abe K, Vonk Noordegraaf A, Voelkel NF (2009) The right ventricle under pressure: cellular and molecular mechanisms of right-heart failure in pulmonary hypertension. *Chest* 135:794–804
 19. Phan D, Rasmussen TL, Nakagawa O, McAnally J, Gottlieb PD, Tucker PW, Richardson JA, Bassel-Duby R, Olson EN (2005) BOP, a regulator of right ventricular heart development, is a direct transcriptional target of MEF2C in the developing heart. *Development* 132:2669–2678
 20. Zeisberg EM, Ma Q, Juraszek AL, Moses K, Schwartz RJ, Izumo S, Pu WT (2005) Morphogenesis of the right ventricle requires myocardial expression of Gata4. *J Clin Invest* 115:1522–1531
 21. Louie EK, Rich S, Levitsky S, Brundage B (1992) Doppler echocardiographic demonstration of the differential effects of right ventricular pressure and volume overload on left ventricular geometry and filling. *J Am Coll Cardiol* 19:84–90
 22. Santamore WP, Dell'Italia LJ (1998) Ventricular interdependence: significant left ventricular contributions to right ventricular systolic function. *Prog Cardiovasc Dis* 40:289–308
 23. Oh JK, Hatle LK, Seward JB, Danielson GK, Schaff HV, Reeder GS, Tajik AJ (1994) Diagnostic role of Doppler echocardiography in constrictive pericarditis. *J Am Coll Cardiol* 23:154–162
 24. Torrent-Guasp F, Ballester M, Buckberg GD, Carreras F, Flotats A, Carrio I, Ferreira A, Samuels LE, Narula J (2001) Spatial orientation of the ventricular muscle band: physiologic contribution and surgical implications. *J Thorac Cardiovasc Surg* 122:389–392
 25. Buckberg GD, Coghlan HC, Torrent-Guasp F (2001) The structure and function of the helical heart and its buttress wrapping. V. Anatomic and physiologic considerations in the healthy and failing heart. *Semin Thorac Cardiovasc Surg* 13:358–385
 26. Torrent-Guasp F, Kocica MJ, Corno AF, Komeda M, Carreras-Costa F, Flotats A, Cosin-Aguillar J, Wen H (2005) Towards new understanding of the heart structure and function. *Eur J Cardio-thor Surg* 27:191–201
 27. King ME, Braun H, Goldblatt A, Liberthson R, Weyman AE (1983) Interventricular septal configuration as a predictor of right ventricular systolic hypertension in children: a cross-sectional echocardiographic study. *Circulation* 68:68–75
 28. Dellegrottaglie S, Sanz J, Poon M, Viles-Gonzalez JF, Sulica R, Goyenechea M, Macaluso F, Valentin Fuster RT, Rajagopalan S (2007) Pulmonary hypertension: accuracy of detection with left ventricular septal-to-free wall curvature ratio measured at cardiac MR. *Radiology* 243:63–69
 29. Flachskampf FA, Voigt JU (2005) The interventricular septum is functionally bilayered: a fresh look at a well known structure. *Heart* 91:1260–1261
 30. Li KS, Santamore WP (1993) Contribution of each wall to biventricular function. *Cardiovasc Res* 27:792–800
 31. Beyar R, Dong SJ, Smith ER, Belenkie I, Tyberg JV (1993) Ventricular interaction and septal deformation: a model compared with experimental data. *Am J Physiol* 265:H2044–H2056
 32. Boettler P, Claus P, Herbots L, McLaughlin M, D'hooge J, Bijns B, Ho SY, Kececioglu D, Sutherland GR (2005) New aspects of the ventricular septum and its function: an echocardiographic study. *Heart* 91:1343–1348
 33. Saleh S, Liakopoulos OJ, Buckberg GD (2006) The septal motor of biventricular function. *Eur J Cardiothorac Surg* 29:126–138
 34. Prakash R (1978) Echocardiographic and necropsy thickness in systole and diastole. Determination of right ventricular wall correlation in 32 patients. *Heart* 40:1257–1261
 35. Foale R, Nihoyannopoulos P, McKenna W, Kleinebenne A, Nadazdin A, Rowland E, Smith G (1986) Echocardiographic measurement of the normal adult right ventricle. *Br Heart J* 56:33–44
 36. Lang RM, Bierig M, Devereux RB, Flachskampf FA, Foster E, Pellikka PA, Picard MH, Roman MJ, Seward J, Shanewise JS, Solomon SD, Spencer KT, Sutton MS, Stewart WJ (2005) Recommendations for chamber quantification: a report from the American society of echocardiography's guidelines and standards committee and the chamber quantification writing group, developed in conjunction with the European association of echocardiography, a branch of the European society of cardiology. *J Am Soc Echocardiogr* 18:1440–1463
 37. Joyce JJ, Denslow S, Kline CH, Baylen BG, Wiles HB (2001) Estimation of right ventricular free-wall mass using two-dimensional echocardiography. *Pediatr Cardiol* 22:306–314
 38. Vieillard-Baron A, Schmitt JM, Augarde R, Fellahi JL, Prin S, Page B, Beauchet A, Jardin F (2001) Acute cor pulmonale in acute respiratory distress syndrome submitted to protective ventilation: incidence, clinical implications, and prognosis. *Crit Care Med* 29:1551–1555
 39. Cohen GI, White M, Sochowski RA, Klein AL, Bridge PD, Stewart WJ, Chan KL (1995) Reference values for normal adult transesophageal echocardiographic measurements. *J Am Soc Echocardiogr* 8:221–230
 40. Kjaergaard J, Petersen CL, Kjaer A, Schaadt BK, Oh JK, Hassager C (2006) Evaluation of right ventricular volume and function by 2D and 3D echocardiography compared to MRI. *Eur J Echocardiogr* 7:430–438
 41. Schenk P, Globits S, Koller J, Brunner C, Artemiou O, Klepetko W, Burghuber OC (2000) Accuracy of echocardiographic right ventricular parameters in patients with different end-stage lung diseases prior to lung transplantation. *J Heart Lung Transplant* 19:145–154
 42. Lai WW, Gauvreau K, Rivera ES, Saleeb S, Powell AJ, Geva T (2008) Accuracy of guideline recommendations for two-

- dimensional quantification of the right ventricle by echocardiography. *Int J Cardiovasc Imaging* 24:691–698
43. Chierrie Y, Barbier G, Feldmann L, Grentzinger A, Danchin N, Chierrie F (1997) Additional predictive value of both left and right ventricular ejection fractions on long-term survival in idiopathic dilated cardiomyopathy. *Eur Heart J* 18:276–280
 44. Lindqvist P, Henein M, Kazzam E (2003) Right ventricular outflow-tract fractional shortening: an applicable measure of right ventricular systolic function. *Eur J Echocardiogr* 4:29–35
 45. Denslow S, Whiles HB (1998) Right ventricular volumes revisited: a simple model and simple formula for echocardiographic determination. *J Am Soc Echocardiogr* 11:864–873
 46. Kovalova S, Necas J, Cerbak R, Malik P, Vespalec J (2005) Echocardiographic volumetry of the right ventricle. *Eur J Echocardiogr* 6:15–23
 47. Lopez-Candales A, Dohi K, Iliescu A, Peterson RC, Edelman K, Bazaz R (2006) An abnormal right ventricular apical angle is indicative of global right ventricular impairment. *Echocardiography* 23:361–368
 48. Anavekar NS, Gerson D, Skali H, Kwong RY, Yucel EK, Solomon SD (2007) Two-dimensional assessment of right ventricular function: an echocardiographic-MRI correlative study. *Echocardiography* 24:452–456
 49. Anavekar NS, Skali H, Bourgoun M, Ghali JK, Kober L, Maggioni AP, McMurray JJV, Velazquez E, Califf R, Pfeffer MA, Solomon SD (2008) Usefulness of right ventricular fractional area change to predict death, heart failure, and stroke following myocardial infarction (from the VALIANT ECHO study). *Am J Cardiol* 101:607–612
 50. Kaul S, Tei C, Hopkins JM, Shah PM (1984) Assessment of right ventricular function using two-dimensional echocardiography. *Am Heart J* 107:526–531
 51. López-Candales A, Rajagopalan N, Saxena N, Gulyasy B, Edelman K, Bazaz R (2006) Right ventricular systolic function is not the sole determinant of tricuspid annular motion. *Am J Cardiol* 98:973–977
 52. Eidem BW, Tei C, O'Leary PW, Cetta F, Seward JB (1998) Nongeometric quantitative assessment of right and left ventricular function: myocardial performance index in normal children and patients with Ebstein anomaly. *J Am Soc Echocardiogr* 11:849–856
 53. Hsiao SH, Yang SH, Wang WC, Lee CY, Lin SK, Liu CP (2006) Usefulness of regional myocardial performance index to diagnose pulmonary embolism in patients with echocardiographic signs of pulmonary hypertension. *Am J Cardiol* 98:1652–1655
 54. Yoshifuku S, Otsuji Y, Takasaki K, Yuge K, Kisanuki A, Toyonaga K, Lee S, Murayama T, Nakashima H, Kumanohoso T, Minagoe S, Tei C (2003) Pseudonormalized Doppler total ejection isovolume (Tei) index in patients with right ventricular acute myocardial infarction. *Am J Cardiol* 91:527–531
 55. Joyce JJ, Chang RK, Qi N, Owens TR, Ginzton LE, Baylen BG (2004) Echocardiographic assessment of the right ventricular stress-velocity relationship under normal and chronic overload conditions. *Echocardiography* 21:17–25
 56. Lee KS, Abbas AE, Khandheria BK, Lester SJ (2007) Echocardiographic assessment of right heart hemodynamic parameters. *J Am Soc Echocardiogr* 20:773–782
 57. Collins N, Bastian B, Quiqueree L, Jones C, Morgan R, Reeves G (2006) Abnormal pulmonary vascular responses in patients registered with a systemic autoimmunity database: pulmonary hypertension assessment and screening evaluation using stress echocardiography (Phase—I). *Eur J Echocardiogr* 7:439–446
 58. Barst RJ, Langleben D, Frost A, Horn EM, Oudiz R, Shapiro S, McLaughlin V, Hill N, Tapson VF, Robbins IM, Zwicke D, Duncan B, Dixon RA, Frumkin LR (2004) STRIDE-1 study group. Sitaxsentan therapy for pulmonary arterial hypertension. *Am J Respir Crit Care Med* 169:441–447
 59. Sun Y, Belenkie I, Wang JJ, Tyberg JV (2006) Assessment of right ventricular diastolic suction in dogs with the use of wave intensity analysis. *Am J Physiol Heart Circ Physiol* 291:H3114–H3121
 60. Klein AL, Leung DY, Murray D, Urban LH, Bailey KR, Tajik AJ (1999) Effects of age and physiologic variables on right ventricular filling dynamics in normal subjects. *Am J Cardiol* 84:440–448
 61. Nakamura K, Miyahara Y, Ikeda S, Naito T (1995) Assessment of right ventricular diastolic function by pulsed Doppler echocardiography in chronic pulmonary disease and pulmonary thromboembolism. *Respiration* 62:237–243
 62. Burgess MI, Mogulkoc N, Bright-Thomas RJ, Bishop P, Egan JJ, Ray SG (2002) Comparison of echocardiographic markers of right ventricular function in determining prognosis in chronic pulmonary disease. *J Am Soc Echocardiogr* 15:633–639
 63. Nath J, Vacek JL, Heidenreich PA (2006) A dilated inferior vena cava is a marker of poor survival. *Am Heart J* 151:730–735
 64. Gaynor SL, Maniar HS, Bloch JB, Steendijk P, Moon MR (2005) Right atrial and ventricular adaptation to chronic right ventricular pressure overload. *Circulation* 112(1):1
 65. Lindqvist P, Waldenstrom A, Henein M, Morner S, Kazzam E (2005) Regional and global right ventricular function in healthy individuals aged 20–90 years: a pulsed Doppler tissue imaging study. *Echocardiography* 22:305–314
 66. Drighil A, Madias JE, Mathewson JW, El Mosalami H, El Badaoui N, Ramdani B, Bennis A (2008) Haemodialysis: effects of acute decrease in preload on tissue Doppler imaging indices of systolic and diastolic function of the left and right ventricles. *Eur J Echocardiogr* 9(4):530–535
 67. Boissiere J, Gautier M, Machet MC, Hanton G, Bonnet P, Eder V (2005) Doppler tissue imaging in assessment of pulmonary hypertension induced right ventricle dysfunction. *Am J Physiol Heart Circ Physiol* 289:H2450–H2455
 68. Nageh MF, Kopelen HA, Zoghbi WA, Quiñones MA, Nagueh SF (1999) Estimation of mean right atrial pressure using tissue Doppler imaging. *Am J Cardiol* 84:1448–1451
 69. Sade LE, Gulmez O, Eroglu S, Sezgin A, Muderrisoglu H (2007) Noninvasive estimation of right ventricular filling pressure by ratio of early tricuspid inflow to annular diastolic velocity in patients with and without recent cardiac surgery. *J Am Soc Echocardiogr* 20:982–988
 70. Shiina Y, Funabashi N, Lee K, Daimon M, Sekine T, Kawakubo M, Takahashi M, Yajima R, Tanabe N, Kuriyama T, Komuro I (2009) Right atrium contractility and right ventricular diastolic function assessed by pulsed tissue Doppler imaging can predict brain natriuretic peptide in adults with acquired pulmonary hypertension. *Int J Cardiol* 135:53–59
 71. Lewis JF, Webber JD, Sutton LL, Chesoni S, Curry CL (1993) Discordance in degree of right and left ventricular dilation in patients with dilated cardiomyopathy: recognition and clinical implications. *J Am Coll Cardiol* 21:649–654
 72. La Vecchia L, Paccanaro M, Bonanno C, Varotto L, Ometto R, Vincenzi M (1999) Left ventricular versus biventricular dysfunction in idiopathic dilated cardiomyopathy. *Am J Cardiol* 83:120–122
 73. Yu HC, Sanderson JE (1999) Different prognostic significance of right and left ventricular diastolic dysfunction in heart failure. *Clin Cardiol* 22:504–512
 74. Nesser HJ, Tkalec W, Patel AR, Masani ND, Niel J, Markt B, Pandian NG (2006) Quantitation of right ventricular volumes and ejection fraction by three-dimensional echocardiography in patients: comparison with magnetic resonance imaging and radionuclide ventriculography. *Echocardiography* 23:666–680

75. Niemann PS, Pinho L, Balbach T, Galuschky C, Blankenhagen M, Silberbach M, Broberg C, Jerosch-Herold M, Sahn DJ (2007) Anatomically oriented right ventricular volume measurements with dynamic three-dimensional echocardiography validated by 3-tesla magnetic resonance imaging. *J Am Coll Cardiol* 50:1668–1676
76. Tamborini G, Brusoni D, Torres Molina JE, Galli CA, Maltagliati A, Muratori M, Susini F, Colombo C, Maffessanti F, Pepi M (2008) Feasibility of a new generation three-dimensional echocardiography for right ventricular volumetric and functional measurements. *Am J Cardiol* 102:499–505
77. Kukulski T, Hübbert L, Arnold M, Wranne B, Hatle L, Sutherland GR (2000) Normal regional right ventricular function and its change with age: a Doppler myocardial imaging study. *J Am Soc Echocardiogr* 13:194–204
78. Kjaergaard J, Sogaard P, Hassager C (2006) Quantitative echocardiographic analysis of the right ventricle in healthy individuals. *J Am Soc Echocardiogr* 19:1365–1372
79. Meluzin J, Spinarova L, Bakala J, Toman J, Krejci J, Hude P, Kára T, Soucek M (2001) Pulsed Doppler tissue imaging of the velocity of tricuspid annular systolic motion; a new, rapid, and non-invasive method of evaluating right ventricular systolic function. *Eur Heart J* 22:340–348
80. Lindqvist P, Caidahl K, Neuman-Andersen G, Ozolins C, Rantapaa-Dahlqvist S, Waldenstrom A, Kazzam E (2005) Disturbed right ventricular diastolic function in patients with systemic sclerosis: a Doppler tissue imaging study. *Chest* 128:755–763
81. Tugcu A, Guzel D, Yildirimturk O, Aytakin S (2009) Evaluation of right ventricular systolic and diastolic function in patients with newly diagnosed obstructive sleep apnea syndrome. *Cardiology* 113:184–192
82. Dokainish H, Sengupta R, Patel R, Lakkis N (2007) Usefulness of right ventricular tissue Doppler imaging to predict outcome in left ventricular heart failure independent of left ventricular diastolic function. *Am J Cardiol* 99:961–965
83. David J-S, Tousignant CP, Bowry R (2006) Tricuspid annular velocity in patients undergoing cardiac operation using transesophageal echocardiography. *J Am Soc Echocardiogr* 19:329–334
84. Sade LE, Gülmez O, Ozyer U, Özgül E, Ağildere M, Müderrisoğlu H (2009) Tissue Doppler study of the right ventricle with a multisegmental approach: comparison with cardiac magnetic resonance imaging. *J Am Soc Echocardiogr* 22:361–368
85. Roberson DA, Cui W (2007) Right ventricular Tei index in children: effect of method, age, body surface area, and heart rate. *J Am Soc Echocardiogr* 20:764–770
86. Blanchard DG, Malouf PJ, Gurudevan SV, Auger WR, Madani MM, Thistlethwaite P, Waltman TJ, Daniels LB, Raisinghani AB, DeMaria AN (2009) Utility of right ventricular Tei index in the noninvasive evaluation of chronic thromboembolic pulmonary hypertension before and after pulmonary thromboendarterectomy. *JACC Cardiovasc Imag* 2:143–149
87. Vogel M, Schmidt MR, Kristiansen SB, Cheung M, White PA, Sorensen K, Redington AN (2002) Validation of myocardial acceleration during isovolumic contraction as a novel noninvasive index of right ventricular contractility: comparison with ventricular pressure-volume relations in an animal model. *Circulation* 105:1693–1699
88. Vogel M (2004) Systemic ventricular function in patients with transposition of the great arteries after atrial repair: a tissue Doppler and conductance catheter study. *J Am Coll Cardiol* 43:100–106
89. Frigiola A, Redington AN, Cullen S, Vogel M (2004) Pulmonary regurgitation is an important determinant of right ventricular contractile dysfunction in patients with surgically repaired tetralogy of Fallot. *Circulation* 110:II153–II157
90. Kjaergaard J, Snyder EM, Hassager C, Oh JK, Johnson BD (2006) Impact of preload and afterload on global and regional right ventricular function and pressure: a quantitative echocardiography study. *J Am Soc Echocardiogr* 19:515–521
91. Lindqvist P, Waldenstrom A, Wikstrom G, Kazzam E (2006) Right ventricular myocardial isovolumic relaxation time and pulmonary pressure. Pulsed Doppler tissue imaging in resurrector of Burstin's nomogram. *Clin Physiol Funct Imaging* 26:1–8
92. Ramzy IS, O'Sullivan CA, Lam Y, Dancy M, Tei C, Henein MY (2009) Right ventricular stunning in inferior myocardial infarction. *Int J Cardiol* 136:294–299
93. Dubin AM, Janousek J, Rhee E, Strieper MJ, Cecchin F, Law IH, Shannon KM, Temple J, Rosenthal E, Zimmerman FJ, Davis A, Karpawich PP, Al Ahmad A, Vetter VL, Kertesz NJ, Shah M, Snyder C, Stephenson E, Emmel M, Sanatani S, Kanter R, Batra A, Collins KK (2005) Resynchronization therapy in pediatric and congenital heart disease patients: an international multicenter study. *J Am Coll Cardiol* 46:2277–2283
94. Rajagopalan N, Dohi K, Simon MA, Suffoletto M, Edelman K, Murali S, Lopez-Candales A (2006) Right ventricular dyssynchrony in heart failure: a tissue Doppler imaging study. *J Card Failure* 12:263–267
95. Donal E, Thibault H, Bergerot C, Leroux PY, Cannesson M, Thivolet S, Barthelet M, Rivard L, Chevalier P, Ovize M, Daubert JC, Leclercq C, Mabo P, Derumeaux G (2008) Right ventricular pump function after cardiac resynchronization therapy: a strain imaging study. *Arch Cardiovasc Dis* 101:475–484
96. Vitarelli A, Franciosa P, Conde Y, D'Orazio S, Stellato S, Battaglia D, Caranci F, Continanza G, Dettori O, Capotosto L, Rosanio S (2009) Quantitative assessment of left and right ventricular dyssynchrony by tissue Doppler and speckle tracking imaging before and after cardiac resynchronization therapy. *Eur J Heart Failure* 8(Suppl):461(abstr)
97. Kowalski M, Kukulski T, Jamal F, D'hooge J, Weidemann F, Rademakers F, Bijmens B, Hatle L, Sutherland GR (2001) Can natural strain and strain rate quantify regional myocardial deformation? A study in healthy subjects. *Ultrasound Med Biol* 27:1087–1097
98. Gondi S, Dokainish H (2007) Right ventricular tissue Doppler and strain imaging: ready for clinical use? *Echocardiography* 24:522–532
99. Donal E, Roulaud M, Raud-Raynier P, De Bisschop C, Leclercq C, Derumeaux G, Daubert JC, Mabo P, Denjean A (2007) Echocardiographic right ventricular strain analysis in chronic heart failure. *Eur J Echocardiogr* 8:449–456
100. Pettersen E, Helle-Valle T, Edvardsen T, Lindberg H, Smith HJ, Smevik B, Smiseth OA, Andersen K (2007) Contraction pattern of the systemic right ventricle. *J Am Coll Cardiol* 49:2450–2456
101. Jamal F, Bergerot C, Argaud L, Loufouat J, Ovize M (2003) Longitudinal strain quantitates regional right ventricular contractile function. *Am J Physiol Heart Circ Physiol* 285:H2842–H2847
102. Missant C, Rex S, Claus P, Mertens L, Wouters PF (2008) Load-sensitivity of regional tissue deformation in the right ventricle: isovolumic versus ejection-phase indices of contractility. *Heart* 94:e15
103. Dambrauskaitė V, Herbots L, Claus P, Verleden G, Van Raemdonck D, Delcroix M, Sutherland GR (2003) Differential changes in regional right ventricular function before and after a bilateral lung transplantation: an ultrasonic strain and strain rate study. *J Am Soc Echocardiogr* 16:432–436
104. Vitarelli A, Conde Y, Cimino E, Stellato S, D'Orazio S, D'Angeli I, Nguyen BL, Padella V, Caranci F, Petroianni A, D'Antoni L, Terzano C (2006) Assessment of right ventricular function by strain Doppler echocardiography in patients with chronic obstructive pulmonary disease. *Eur Respir J* 27:268–275

105. Dambrauskaitė V, Delcroix M, Claus P, Herbots L, D'hooge J, Bijmens B, Rademakers F, Sutherland GR (2007) Regional right ventricular dysfunction in chronic pulmonary hypertension. *J Am Soc Echocardiogr* 10:1172–1180
106. Casazza F, Bongarzone A, Capozzi A, Agostoni O (2005) Regional right ventricular dysfunction in acute pulmonary embolism and right ventricular infarction. *Eur J Echocardiogr* 6:11–14
107. Kjaergaard J, Sogaard P, Hassager C (2004) Right ventricular strain in pulmonary embolism by Doppler tissue echocardiography. *J Am Soc Echocardiogr* 17:1210–1212
108. Pirat B, McCulloch ML, Zoghbi WA (2006) Evaluation of global and regional right ventricular systolic function in patients with pulmonary hypertension using a novel speckle tracking method. *Am J Cardiol* 98:699–704
109. Korinek J, Kjaergaard J, Sengupta PP, Yoshifuku S, McMahon EM, Cha SS et al (2007) High spatial resolution speckle tracking improves accuracy of 2-dimensional strain measurements: an update on a new method in functional echocardiography. *J Am Soc Echocardiogr* 20:165–170
110. Vitarelli A, Cortes Morichetti M, Franciosa P, Stellato S, D'Orazio S, Capotosto L, Vitarelli M, Bernardi M (2008) Assessment of arrhythmogenic right ventricular dysplasia by tissue Doppler and speckle tracking imaging. *Eur J Echocardiogr* 9(Suppl):S40
111. Teske AJ, De Boeck BWL, Olimulder M, Prakken NH, Doevendans PAF, Cramer MJ (2008) Echocardiographic assessment of regional right ventricular function: a head-to-head comparison between 2-dimensional and tissue Doppler-derived strain analysis. *J Am Soc Echocardiogr* 21:275–283
112. Gustafsson U, Lindqvist P, Waldenström A (2008) Apical circumferential motion of the right and the left ventricles in healthy subjects described with speckle tracking. *J Am Soc Echocardiogr* 21:1326–1330
113. Jategaonkar SR, Scholtz W, Butz T, Bogunovic N, Faber L, Horstkotte D (2009) Two-dimensional strain and strain rate imaging of the right ventricle in adult patients before and after percutaneous closure of atrial septal defects. *Eur J Echocardiogr* 10:499–502
114. Chow PC, Liang XC, Cheung EWY, Lam WWM, Cheung XF (2008) New two-dimensional global longitudinal strain and strain rate imaging for assessment of systemic right ventricular function. *Heart* 94:855–859
115. Kutty S, Deatsman SL, Melodee L, Nugent ML, Russell D, Frommelt PC (2008) Assessment of regional right ventricular velocities, strain, and displacement in normal children using velocity vector imaging. *Echocardiography* 25:294–307
116. Friedberg MK, Mertens L (2009) Tissue velocities, strain, and strain rate for echocardiographic assessment of ventricular function in congenital heart disease. *Eur J Echocardiogr* 10:585–593
117. Van de Veire NR, Yu C-M, Ajmone-Marsan N, Bleeker GB, Ypenburg C, De Sutter J, Zhang Q, Fung JWH, Chan JYS, Holman ER, van der Wall EE, Schalij MJ, Bax JJ (2008) Triplane tissue Doppler imaging: a novel three-dimensional imaging modality that predicts reverse left ventricular remodelling after cardiac resynchronisation therapy. *Heart* 94:e9
118. Van de Veire NR, De Sutter J, Bax JJ, Roelandt JRTC (2008) Technological advances in tissue Doppler imaging echocardiography. *Heart* 94:1065–1074
119. Kawagishi T (2008) Speckle tracking for assessment of cardiac motion and dyssynchrony. *Echocardiography* 25:1167–1171
120. Elen A, Choi HF, Loeckx D, Gao H, Claus P, Suetens P, Maes F, D'hooge J (2008) Three-dimensional cardiac strain estimation using spatio-temporal elastic registration of ultrasound images: a feasibility study. *IEEE Trans Med Imag* 27:1580–1591
121. Massie B, Kramer BL, Topic N, Henderson SG (1982) Hemodynamic and radionuclide effects of acute captopril therapy for heart failure: changes in left and right ventricular volumes and function at rest and during exercise. *Circulation* 65:1374–1381
122. Quaipe RA, Christian PE, Gilbert EM, Datz FL, Volkman K, Bristow MR (1998) Effects of carvedilol on right ventricular function in chronic heart failure. *Am J Cardiol* 81:247–250
123. Dore A, Houde C, Chan KL, Ducharme A, Khairy P, Juneau M, Marcotte F, Mercier LA (2005) Angiotensin receptor blockade and exercise capacity in adults with systemic right ventricles: a multicenter, randomized, placebo-controlled clinical trial. *Circulation* 112:2411–2416
124. Provencher S, Herve P, Jais X, Lebrec D, Humbert M, Simonneau G, Sitbon O (2006) Deleterious effects of beta-blockers on exercise capacity and hemodynamics in patients with portopulmonary hypertension. *Gastroenterology* 130:120–126
125. Rich S, Seidlitz M, Dodin E, Osimani D, Judd D, Genthner D, McLaughlin V, Francis G (1998) The short-term effects of digoxin in patients with right ventricular dysfunction from pulmonary hypertension. *Chest* 114:787–792
126. Mathur PN, Powles P, Pugsley SO, McEwan MP, Campbell EJ (1981) Effect of digoxin on right ventricular function in severe chronic airflow obstruction: a controlled clinical trial. *Ann Intern Med* 95:283–288
127. Inglessis I, Shin JT, Lepore JJ, Palacios IF, Zapol WM, Bloch KD, Semigran MJ (2004) Hemodynamic effects of inhaled nitric oxide in right ventricular myocardial infarction and cardiogenic shock. *J Am Coll Cardiol* 44:793–798
128. Yilmaz MB, Yontar CA, Erdem A, Karadas F, Yalta K, Turgut OO, Yilmaz A, Tandogan I (2009) Comparative effects of levosimendan and dobutamine on right ventricular function in patients with biventricular heart failure. *Heart Vessels* 24:16–21
129. Vieillard-Baron A, Jardin F (2003) Why protect the right ventricle in patients with acute respiratory distress syndrome? *Curr Opin Crit Care* 9:15–21
130. Vargas F, Gruson D, Valentino R, Bui HN, Salmi LR, Gilleron V, Gbikpi-Benissan G, Guenard H, Hilbert G (2004) Transesophageal pulsed Doppler echocardiography of pulmonary venous flow to assess left ventricular filling pressure in ventilated patients with acute respiratory distress syndrome. *J Crit Care* 19:187–197
131. Borges AC, Knebel F, Eddicks S, Panda A, Schattke S, Witt C, Baumann G (2006) Right ventricular function assessed by two-dimensional strain and tissue Doppler echocardiography in patients with pulmonary arterial hypertension and effect of vasodilator therapy. *Am J Cardiol* 98:530–534
132. Galie N, Hinderliter AL, Torbicki A, Fourme T, Simonneau G, Pulido T, Espinola-Zavaleta N, Rocchi G, Manes A, Frantz R, Kurzyna M, Nagueh SF, Barst R, Channick R, Dujardin K, Kronenberg A, Leconte I, Rainisio M, Rubin L (2003) Effects of the oral endothelin-receptor antagonist bosentan on echocardiographic and Doppler measures in patients with pulmonary arterial hypertension. *J Am Coll Cardiol* 41:1380–1386
133. Chin KM, Kingman M, de Lemos JA, Warner JJ, Reimold S, Peshock R, Torres F (2008) Changes in right ventricular structure and function assessed using cardiac magnetic resonance imaging in bosentan-treated patients with pulmonary arterial hypertension. *Am J Cardiol* 101:1669–1672
134. Duffels MG, Hardziyenka M, Surie S, de Bruin-Bon RH, Hoendermis ES, van Dijk AP, Bouma BJ, Tan HL, Berger RM, Bresser P, Mulder BJ (2008) Duration of right ventricular contraction predicts the efficacy of bosentan treatment in patients with pulmonary hypertension. *Eur J Echocardiogr* 10:433–438
135. Amaki M, Nakatani S, Kanzaki H, Kyotani S, Nakanishi N, Shigemasa C, Hisatome I, Kitakaze M (2009) Usefulness of three-dimensional echocardiography in assessing right ventricular

- function in patients with primary pulmonary hypertension. *Hypertens Res* 32:419–422
136. Vitarelli A, Conde Y, D’Orazio S, Stellato S, Continanza G, Capotosto L, Salsano F, Terzano C (2008) Strain rate echocardiographic assessment of right ventricular performance in pulmonary arterial hypertension. *Eur J Echocardiogr* 9:S53 (abstr)
137. Ghez O, Tsang VT, Frigiola A, Coats L, Taylor A, Van Doorn C, Bonhoeffer P, De Leval M (2007) Right ventricular outflow tract reconstruction for pulmonary regurgitation after repair of tetralogy of fallot: preliminary results. *Eur J Cardiothorac Surg* 31:654–658
138. Buckberg GD (2006) RESTORE group. Tenth RESTORE group meeting: overview. *Eur J Cardiothorac Surg* 29:213–221
139. Buckberg GD (2007) Congestive heart failure: treat the disease, not the symptom: return to normalcy/part II—the experimental approach. *Eur J Cardiothorac Surg* 134:844–849